

Evaluating a modified point-based method to downscale cell-based climate variable data to high-resolution grids

Alan V. Di Vittorio^{a,b,*} and Norman L. Miller^{b,c}

^aEnergy Biosciences Institute, University of California, Berkeley

^bEarth Sciences Division, Lawrence Berkeley National Laboratory

^cDepartment of Geography, University of California, Berkeley

*Corresponding author; avdivittorio@lbl.gov, 510-486-7798

Mailing address:

Lawrence Berkeley National Laboratory

Earth Sciences Division

One Cyclotron Road, Mail Stop 84R0171

Berkeley, CA 94720-8268

Abstract

To address the demand for high spatial resolution gridded climate data we have advanced the Daymet point-based interpolation algorithm for downscaling global, coarsely gridded data with additional output variables. The updated algorithm, High Resolution Climate Downscaler (HRCDC), performs very good downscaling of daily, global, historical reanalysis data from 1° input resolution to 2.5 arcmin output resolution for day length, downward longwave radiation, pressure, maximum and minimum temperature, and vapor pressure deficit. It gives good results for monthly and yearly cumulative precipitation and fair results for wind speed distributions and modeled downward shortwave radiation. Over complex terrain 2.5 arcmin resolution is likely too low and aggregating it up to 15 arcmin preserves accuracy. HRCDC performs comparably to existing daily and monthly United States data sets but with a global extent for nine daily climate variables spanning 1948-2006. Furthermore, HRCDC can readily be applied to other gridded climate data sets.

Keywords: climate, downscaling; Daymet; grid; HRCDC; PRISM

Abbreviations: DAY, day length; LWRAD, downward long wave radiation; PRCP, precipitation; PRES, surface pressure; RH, relative humidity; SH, specific humidity; SWRAD, downward shortwave radiation; TAVG, average air temperature; TDAY, average daytime temperature; TDEW, dew point temperature; TMAX, maximum temperature; TMIN, minimum temperature; VPD, vapor pressure deficit; WND, wind speed; HRCDC, high resolution climate downscaler

1. Introduction

Many applications and research disciplines, including ecosystem modeling (Di Vittorio et al. 2010; Kucharik et al. 2000; Miguez et al. 2009), hydrologic assessment (Anandhi et al. 2008), land conservation (Bayliss et al. 2005; Cabeza et al. 2010; Galatowitsch et al. 2009), and regional planning and decision-making (Girvetz et al. 2008), require high spatial resolution, gridded input climate data with daily or hourly frequency. Ecosystem models generally have daily (Di Vittorio et al. 2010; Running and Coughlan 1988; Thornton and Rosenbloom 2005) or sub-daily (Kucharik et al. 2000; Miguez et al. 2009) time steps, and many regional applications need high spatial resolution with length scales less than 1 km. Regions with dramatic terrain variations especially require sufficiently high spatial resolution to properly represent topographic microclimate effects (Daly et al. 1994; Steinacker et al. 2006; Thornton et al. 1997). Also, many ecosystem models often require radiation, humidity, and wind speed data, in addition to more commonly available temperature and precipitation data (Di Vittorio et al. 2010; Kucharik et al. 2000; Running and Coughlan 1988; Thornton and Rosenbloom 2005).

Many archived global climate data sets have high temporal frequency (≤ 1 day), but very coarse spatial resolution, such as the $1^\circ \times 1^\circ$ surface data maintained by the Land Surface Hydrology Research Group (LSHRG) at Princeton University (Sheffield et al. 2006) and the $2.5^\circ \times 2.5^\circ$ National Centers for Environmental Prediction (NCEP)/National Center for Atmospheric Research (NCAR) reanalysis data (Kalnay et al. 1996). The North American Regional Reanalysis (NARR) data set has $1/3^\circ \times 1/3^\circ$ resolution for North America only (Mesinger et al. 2006). Monthly global data sets at $0.5^\circ \times 0.5^\circ$ resolution (Mitchell and Jones 2005) and 50-year average

monthly climatology data at 30 arcsec resolution also exist (WorldClim, Hijmans et al. 2005). Monthly temperature and precipitation data interpolated by the Parameter-elevation Regressions on Independent Slopes Model (PRISM) are also available for the U.S. from 1971 to present at 2.5 arcmin resolution (Daly et al. 2002).

Due to insufficient spatial and temporal data for current research and applications, many methods exist to downscale coarse resolution climate fields. Such methods fall into two categories: dynamical or statistical (Giorgi et al. 1994; Hewitson and Crane 1996; Miller et al. 2009; Wilby and Wigley 1997). Dynamical downscaling is physically based and utilizes Regional Climate Models (RCMs) with high computational requirements (Lo et al. 2008; Sylla et al. 2009). RCMs are more robust than statistical methods, but to date they do not give significantly better results for temperature and precipitation and are considered too expensive for operational use (Salathe et al. 2007; Spak et al. 2007). Statistical methods are computationally inexpensive, assume stationarity in predictor-predictand relationships, require robust relationships among sufficient data, are vulnerable to data error and omitted dependencies, and generally focus on precipitation and/or temperature (Anandhi et al. 2008; Boé et al. 2007; Charles et al. 1999; Cheng et al. 2008; Landman and Tennant 2000; Maurer et al. 2010; Schubert 1998; Trigo and Palutikof 2001; Wilby et al. 1998; Zhang 2005). These statistical methods rely on relationships between coarsely gridded reanalysis or Global Circulation Model (GCM) data, and point or fine-scale gridded observations. These relationships are calculated for a calibration period, validated for a separate time period, and then applied to other time periods, with the assumption of temporal stationarity. Charles et al. (1999) found that this stationary assumption is

not sound, and Paul et al. (2008) tried to circumvent this stationary requirement, but was only able to show that GCM projections carry their historic mean statistical properties forward in time.

The statistical interpolation of gridded climate data from irregularly spaced point data also aims to produce high spatial resolution grids, but is generally applied to observations. These statistical methods do not assume temporal stationarity and have method-dependent assumptions for spatial stationarity. Daly et al. (1994) and Thornton et al. (1997) reviewed the history of statistical techniques from linear interpolation to kriging and found that simple techniques often produce the best results with greatest efficiency. Daly et al. (2002) combined statistical interpolation with topography-based area partitioning and expert knowledge to generate monthly precipitation, and maximum, minimum and dew point temperature grids over the conterminous U.S. at 2.5 arcmin resolution. Maurer et al. (2002) used a combination of simple regression methods similar to the Daymet algorithm (Thornton et al. 1997), an area partitioning method (Shepard, 1968), and a weather generator to obtain a $1/8^\circ$ resolution grid of six climate variables (precipitation, temperature, downward shortwave and longwave radiation, vapor pressure deficit, and wind) for the conterminous U.S. at 3-hourly time steps. Steinacker et al. (2006) used a ‘topographic fingerprint’ method to determine mesoscale pressure fields across Europe at 10 km resolution.

With modification and the use of spatially contiguous variables (e.g. elevation) these interpolation techniques have the potential to robustly downscale coarsely gridded climate data without the main assumption of temporal stationarity. Interpolation-based techniques would

obviate the need for this assumption because they would develop statistical relationships at each time step between coarse-resolution climate data and relatively constant physical predictors, such as topography. These relationships would then be applied directly to high-resolution topography to obtain downscaled climate data. Terrain is not the only determinant of climate variables (e.g. wind advection and precipitation), but reliable high-resolution elevation data and known relationships between topography and climate create possibilities for interpolation-based downscaling techniques for terrain sensitive variables. To our knowledge the application of interpolation methods to gridded data has been limited to resampling for georectification (Aronoff 2005; Jensen 2005; Richards 1993), with the exception of some applications of fractal interpolation to precipitation (Tao and Barros 2010).

A major challenge for all methods is the discrepancy between point and area data, often classified as a type of scale mismatch. Dynamic downscaling generates gridded data that represent averages of processes occurring within each grid cell area. This raises the question of how well a particular resolution grid represents a smaller area or unevenly distributed point data within grid cells. Statistical downscaling is bound to either area or point observation data depending on which was used to develop the transfer functions. Interpolation methods employ weighted point data to estimate gridded values (Daly et al. 2002; Maurer et al. 2002). In this case the issue is how well point data represents grid cell areas and how many interpolated point values are needed to obtain sufficiently reliable gridded data. Applying interpolation methods to gridded data creates additional concerns regarding the location of the input value within its grid cell.

Point-versus-cell uncertainties are very important for developing and evaluating accurate

high spatial resolution grids. Tustison et al. (2001) formalized the uncertainty associated with such scale mismatch as 'representativeness error', and indicated that it is scale dependent and can be greater than 50% of the regional mean of the underlying, high-resolution field. This scale dependency arises for a variety of reasons. A coarse grid (e.g. $1^\circ \times 1^\circ$) is expected to yield only a general trend primarily because there is no representation of the sub-grid spatial heterogeneity. On the other hand, fine-grained grids capture spatial heterogeneity through representation of small uniform areas, resulting in grids that are more sensitive to heterogeneities than coarse grids. Neighboring grid cells are likely to cover similar areas, and a spatially anomalous feature can be, among other possibilities, adequately represented if it dominates a grid cell, or a source of error if it is only a small part of the grid cell and is used to characterize the entire grid cell.

We address the following questions by evaluating a statistical interpolation method (Thornton et al. 1997) we advanced and implemented to downscale global, gridded data for driving an agro-ecosystem model (Di Vittorio et al. 2010) at high resolution:

- How do we best apply simple point interpolation methods to gridded data?
- What limits the output grid resolution and how does temporal averaging influence downscaled accuracies?
- How do downscaled grid accuracies calculated with respect to point observations compare with accuracies calculated with respect to gridded data?

Hereafter we refer to this downscaling method as the High Resolution Climate Downscaler (HRCDC). The main goal of HRCDC is to provide high-resolution, global meteorological forcing data for terrestrial applications, without assuming temporal stationarity. Section 2 describes our

downscaling algorithm, input and verification data, output climate data, and statistical analyses. Section 3 presents comparisons between evaluations of HRCD, Daymet, and PRISM against site observations, comparisons between evaluations of HRCD and Daymet against PRISM cells containing sites, evaluation of HRCD against PRISM for a $5^\circ \times 5^\circ$ extent grid, and evaluations of aggregated HRCD and PRISM grid cells against two sites. Section 4 provides a brief discussion of these results, next steps, and concluding remarks.

2. Materials and Methods

2.1 Downscaling algorithm

HRCD is a two-stage algorithm (Figure 1) based on Thornton et al. (1997). The first stage builds a terrain grid with specified output cell size, extent, and projection (geographic or sinusoidal equal area). The second stage interpolates input climate variable data to the terrain grid at each time step, which is daily in this study. We define the center of each output grid cell as the target interpolation point because preliminary analysis has shown that averaging a single-elevation sub-grid within an output cell produces nearly identical results as using a centered interpolation point. Input cell values are also located at their respective cell centers for application of a modified cosine interpolation algorithm (Zhao et al. 2005). HRCD weights all averaging processes by area to produce values representative of output cell areas (Isaaks and Srivastava 1989). Day length is always calculated from latitude and east and west horizon elevation angles. HRCD assumes a spherical earth with radius equal to the World Geodetic System 1984 (WGS84) average earth radius: 6371007.181 m. Using this value is justified

because the estimated cell area error for a spherical earth with respect to a spheroidal earth ranges from 0.22% at the equator to 0.45% at the poles.

2.1.1. Elevation-adjusted interpolation

The HRCD elevation-adjusted interpolation scheme is a modified version of the Daymet algorithm with adapted MT-CLIM 4.3 routines (Kimball et al. 1997; Running et al. 1987; Thornton et al. 2000; Thornton et al. 1997). The original Daymet algorithm uses irregularly spaced input points while HRCD uses gridded input climate data. HRCD retains the general method of calculating linear regressions between point-pair precipitation or temperature differences and point-pair elevation differences. The resulting regression coefficients are then applied at each input cell center, using the difference between the input and output cell elevations to calculate an elevation-adjusted value for each input cell. To obtain an output cell value from adequately weighted, cell-based input data, HRCD replaces Daymet's Gaussian interpolation (Thornton et al. 1997) with a modified cosine interpolation (Appendix A). This method uses only the four nearest-neighbor elevation-adjusted input cell values and favors the input cell containing the output cell.

Additionally, gridded input and output data have different parameterization requirements than point data (Table 1). Spatial smoothing of elevation is unnecessary because elevation values are already averaged for input and output grid cells. Likewise, HRCD does not need to perform temporal smoothing of input temperature and precipitation values because these values already have reduced variability due to large input cell areas. However, we added two parameters—

extreme precipitation threshold (EXTR_PRCP, cm) and maximum precipitation reduction exponent (PRCP_REDUCE, dimensionless)—to correct unrealistically high precipitation estimates. When the elevation-adjusted precipitation (PRCP, cm) value is greater than EXTR_PRCP, HRCD calculates a new precipitation value:

$$PRCP_{new} = MAX_{in} + MAX_{in} * \frac{1}{MAX_{in}^{PRCP_REDUCE}}, \quad (1)$$

where $PRCP_{new}$ is the newly calculated precipitation (cm), MAX_{in} is the maximum input precipitation value used to calculate PRCP (cm), and PRCP_REDUCE is the parameter for reducing the magnitude of MAX_{in} in the denominator of the scaling value (%). $PRCP_{new}$ replaces the elevation-adjusted PRCP only if $PRCP_{new}$ is less than PRCP.

We adjusted all but one of Daymet’s other precipitation and temperature parameter values so they would apply to gridded inputs (Table 1). Thornton et al. (1997) estimated optimal numbers of points and corresponding Gaussian shape parameters for minimizing error when regressing temperature or precipitation differences against elevation differences. We chose similar values by applying their results to fixed-size grid neighborhoods. We did not modify the maximum value for the magnitude of estimated precipitation ratio, and we calibrated the rest of the parameters (Table 1) by comparing HRCD outputs with observations. CRIT_POP, EXTR_PRCP, and PRCP_REDUCE were originally calibrated during HRCD development using the 2001 - 2006 AmeriFlux tower data from Vaira Ranch, CA (38.41°N, 120.95°W; Ma et al. 2007) and National Oceanic and Atmospheric Administration (NOAA) NCDC data from Urbana, IL (40°5’N, 88°14’W). In this study we calibrated EXTR_PRCP, PRCP_REDUCE, and CRIT_POP by adjusting

their values so that downscaled cumulative precipitation and number of precipitation days best matched observations from 17 weather stations from 1998 to 2003 (Table 2). If the fraction of rainy input cells used in the regression is greater than the precipitation occurrence threshold (CRIT_POP, dimensionless), then the output cell will be rainy if at least one of the four nearest neighbor input cells is also rainy. These precipitation parameters affect only PRCP and, indirectly, downward net shortwave radiation (SWRAD, $W m^{-2}$).

HRCDD employs different algorithms based on the availability of particular input variables. The elevation adjustment algorithm regresses differences in cumulative daily PRCP, maximum temperature (TMAX), minimum temperature (TMIN), and—if input data are available—average dew point temperature (TDEW) and average temperature (TAVG) against differences in elevation (m; all temperatures in °C). If humidity data are available then TDEW is downscaled and converted to average vapor pressure deficit (VPD, Pa), then the algorithm calculates SWRAD from terrain, latitude, and actual vapor pressure (Thornton and Running, 1999). Average specific humidity (SH, $kg \text{ water vapor} (kg \text{ total air})^{-1}$) is more commonly available than TDEW, however, and SH is converted to TDEW based on eqns. (B1) – (B2). TDEW is converted to VPD based on eqns. (B1), (B3), and (B4) (Appendix B) If humidity is not available an iterative algorithm estimates TDEW, VPD, and SWRAD from TMIN, average daytime temperature (TDAY), terrain, and latitude (Kimball et al., 1997; Thornton et al., 2000). If input TAVG and average surface pressure (PRES, Pa) data are available HRCDD applies these and the elevation-adjusted TAVG to the hypsometric equation (eqn. B5; Holton 1992) to calculate elevation-adjusted PRES and then converts output VPD to SH based on eqns. (B1) – (B4)

(Appendix B). If TAVG and PRES are not available, then output pressure is estimated as a function of elevation (Iribane and Godson 1981).

2.2. Source data

HRCD uses two different elevation data sets, depending on the output grid resolution and latitude, to calculate five required terrain variables: elevation, slope, aspect, and the vertical angles to east and west horizons. For output grid resolutions finer than 30 arcsec within $\pm 60^\circ$ latitude HRCD uses the 3 arcsec, Consultative Group for International Agriculture Research - Consortium for Spatial Information (CGIAR-CSI) version four corrected Shuttle Radar Topography Mission (SRTM) data set (Jarvis et al., 2008). For all grid resolutions coarser than or equal to 30 arcsec and any grid extending beyond $\pm 60^\circ$ latitude HRCD uses the United States Department of Commerce (USDC) NOAA National Geophysical Data Center (NGDC) Global Land One-kilometer Base Elevation (GLOBE) data set (Hastings and Dunbar 1999). The values in each of these data sets represent average elevations within grid cells.

HRCD uses a globally gridded ($1^\circ \times 1^\circ$) 1948-2006 daily climate variable data set comprising PRCP ($\text{kg H}_2\text{O m}^{-2} \text{s}^{-1}$), TAVG, TMAX and TMIN (K), PRES (Pa), SH, SWRAD (W m^{-2}), average downward net long-wave radiation (LWRAD, W m^{-2}), and average wind speed (WND, m s^{-1}) (Sheffield et al. 2006). These data are maintained by the LSHRG at Princeton University. Additionally, HRCD introduces a systematic bias to input PRCP by integrating over daylight length rather than 24 h. The elevation data (m) associated with these climate data are part of the International Satellite Land Surface Climatology Project (ISLSCP) Initiative II Data

Collection and have recently been added to the LSHRG data set.

2.3. Verification data

We verified HRCD against station-based point data and gridded PRISM data spanning 1998 to 2003. We also compared HRCD and Daymet (Thornton et al. 1997; Daymet accessed 2009) accuracies with respect to these data sets, and compared an aggregated HRCD data set against the input data. The observed point data set comprises 11 stations from the NOAA NCDC cooperative station network and six stations from the NOAA SURFace RADiation (SURFRAD) budget network (Figure 2 and Table 2). These 17 stations represent most climate regimes in the conterminous U.S. and are geographically distributed to provide for a robust evaluation of HRCD.

The NCDC data include daily PRCP (in * 100), WND (mi h⁻¹), and TMAX, TMIN, and TDEW (°F). The SURFRAD data include 3-min temporal averages of the 10 m air temperature (°C), relative humidity (RH, %), PRES (mb), WND (m s⁻¹), SWRAD (W m⁻²), and LWRAD (W m⁻²). We calculated VPD (eqn. B3) for each 3-min interval using 10 m air temperature in place of TDEW to obtain saturation vapor pressure, (e_s , eqn. B1), and using relative humidity (RH) to obtain actual vapor pressure ($e = e_s * RH * 0.01$). VPD was then averaged over daylight length (DAY, s), which was estimated as the diurnal period having positive SWRAD values. We determined TMAX and TMIN for each 24 h period, summed SWRAD over DAY, and averaged WND over DAY.

The gridded data set includes monthly 1998 - 2003 data generated by PRISM (PRISM-

Climate-Group accessed 2010). These data cover the U.S. with 2.5 arcmin resolution and include monthly averages of daily TMAX, TMIN, and TDEW ($^{\circ}\text{C} * 100$) and monthly accumulations of PRCP ($\text{mm} * 100$). We selected the 17 site-containing cells for site-based evaluation. We also selected a $5^{\circ} \times 5^{\circ}$ sub-grid covering part of the southwestern U.S. for grid-based evaluation. The sub-grid covers coastal regions, large inland valleys, desert regions, and extreme topography of the Sierra Nevada and Great Basin (Figure 3; $33^{\circ}33'45''\text{N}$ to $38^{\circ}33'45''\text{N}$ and $115^{\circ}30'75''\text{W}$ to $120^{\circ}30'75''\text{W}$). One NCDC site (Los Angeles, CA) and one SURFRAD site (Desert Rock, NV) are located within the sub-grid. We also aggregated the sub-grid data to seven coarser-resolution grids (Table 3) using area-weighted averaging and only land grid cells.

For comparison with HRCD, the Daymet data set includes daily point data at each of the 17 sites and at the centers of PRISM data cells containing these sites. The PRISM-centered Daymet data represent how a grid might be formed from Daymet point data. These data include TMAX and TMIN ($^{\circ}\text{C}$), PRCP (cm), SWRAD (W m^{-2}), VPD (Pa), and DAY (s).

2.4. Generating HRCD downscaled data sets

To evaluate different configurations of HRCD against verification data, we generated 24 downscaled data sets, 12 that corresponded with the 17 sites and 12 with the $5^{\circ} \times 5^{\circ}$ PRISM sub-grid. The configurations varied with respect to elevation-adjustment, humidity input, precipitation parameters, output cell location and size, and number of interpolation points per output cell. Several configurations did not significantly influence the results (Section 3), so, with respect to verification data, we present only five downscaled data sets and 14 data sets

aggregated from two of these downscaled data sets (Table 3).

We downscaled six years (1998 - 2003) of daily LSHRG data to a 2.5 arcmin resolution grid aligning with the PRISM grid. To minimize computational requirements we performed this downscaling for the 17 cells containing sites (site-based) and for the 5° x 5° PRISM sub-grid (grid-based). The site-based downscaling was performed for two unique sets of precipitation parameters, and both site- and grid-based downscaling was performed using two different HRCD configurations: (1) elevation adjustment with humidity input, and (2) no elevation adjustment (flat-terrain). We aggregated the resulting 5° x 5° grids and the PRISM sub-grid to seven coarser grid resolutions (Table 3), and calculated monthly and annual averages (or totals for precipitation) of daily values.

We also downscaled five different years of daily LSHRG data to each of 11, 4° x 4° grids between 37°N to 41°N; 77°W to 121°W (Table 3). This downscaling was performed with elevation adjustment and humidity input. The westernmost grid includes years 1950 to 1954, each neighboring grid to the east includes the next five years, with the easternmost grid including years 2000 to 2004. The downscaled data were then area-weighted-averaged to match the 1° x 1° LSHRG data, with additional calculations to obtain total monthly PRCP values.

The elevation-adjusted output data comprise DAY, PRCP, PRES, SH, SWRAD, TAVG, TDAY, TMAX, TMIN, and VPD and the flat-terrain output data additionally include LWRAD, SH, and WND. Output TDAY and TAVG were not compared with observations because they are generally not available or are estimated from TMAX and TMIN, as is the case with the NCDC data. Input SH and PRES were used to calculate output VPD, which was then compared with

observations. We did not compare output SH with the SURFRAD data because it is related to VPD. We did, however, evaluate elevation-adjusted PRES because it is required for conversion of output VPD to SH.

2.5. Statistical evaluation

Table 3 shows how the data sets were organized for analysis with respect to verification and source data. The site-based elevation-adjusted data, site-centered Daymet data, and PRISM data were evaluated against site data. The site-based elevation-adjusted data and PRISM-centered Daymet data were evaluated against corresponding PRISM data. The site-based flat-terrain data were evaluated against site data only. The grid-based 2.5 arcmin elevation-adjusted data were evaluated against PRISM data. All 16 flat-terrain and elevation-adjusted grid-based data sets and 8 PRISM sub-grid data sets were evaluated against data from two sites within the specified $5^\circ \times 5^\circ$ extent. PRISM data comparisons include only monthly and yearly TMAX, TMIN, VPD, and PRCP values and all other comparisons additionally include daily values and DAY, PRES, LWRAD, SWRAD, and WND when available.

We performed three levels of statistical analysis for each of HRCD, Daymet, and PRISM, relative to site or PRISM data, by computing the i) Root Mean Squared Error (RMSE) and bias (downscaled mean minus reference mean), and ii) linear regression with student t-test for non-zero slope (significance level $\alpha=0.05$) and the coefficients of determination for the regression model (reg. r^2) and the downscaled data (Goodness of Fit (GOF) R^2). To compare regressions among the data sets, iii) we calculated paired F-tests ($\alpha=0.05$) for regression model slopes and

paired t-tests for bias values ($\alpha=0.05$). We also performed analyses i) and ii) to compare the aggregated HRCD LWRAD, PRCP, TMAX, TMIN, and VPD results with input LSHRG data.

To evaluate the spatial pattern of downscaling error, we subtracted monthly PRISM $5^\circ \times 5^\circ$ sub-grid data from corresponding elevation-adjusted HRCD results to create difference images for PRCP, TMAX, TMIN, and VPD.

3. Results and Discussion

The comparisons in this study demonstrate that HRCD performs well with elevation adjustment and humidity input when the output resolution is fine enough to adequately represent topography (2.5 arcmin or finer). Aggregating 2.5 arcmin output cells to coarser resolutions also produces good results. The original suite of comparison results is very large. Hence, we first provide a summary to specify the sensitivity of HRCD to various configurations, based on the 17 sites, and then present the most relevant results in detail.

We found no statistically significant differences between downscaled values for 3 arcsec site-centered outputs and 2.5 arcmin PRISM-centered outputs. Output resolutions coarser than or equal to 7.5 arcmin produced poor results that did not improve when increasing the number of same-elevation interpolation points within output cells. Using humidity input data increased SWRAD and VPD accuracies over no humidity input, and optimizing precipitation parameters with study site data improved PRCP totals and number of PRCP days with respect to initial parameter values. Elevation adjustment significantly improved relevant output values, which do not include LWRAD and WND, over flat-terrain interpolation. Thus, in the following sections

we present flat-terrain values for LWRAD and WND, and for the other variables we present elevation-adjusted values with humidity input, study-dependent precipitation parameters, and one centered interpolation point per output cell. These HRCD outputs have 2.5 arcmin resolution and align with the PRISM grid, while coarser output resolutions have been aggregated from 2.5 arcmin. The elevation bias for the site-based 2.5 arcmin terrain grid is -0.59 m and only five sites have absolute elevation differences greater than 15 m, with 99 m (26% of the reported site elevation) being the maximum absolute difference (Table 2). Furthermore, the Daymet site- and PRISM-centered data sets have nearly identical accuracies with respect to site-based PRISM data. These results indicate that a 2.5 arcmin HRCD output resolution with one interpolation point per cell is sufficient for characterizing terrain and generating gridded climate variable data representative of these study site locations. More generally, these results show that 2.5 arcmin resolution is sufficient for cell area values to be representative of the point site values, and vice versa.

3.1. Evaluations against site observation data

HRCD produced very good daily data with respect to site observations for DAY, LWRAD, TMAX, TMIN, and VPD (Figure 4 and Table 4). Downscaled daily SWRAD data are fair when compared to observations, and are reasonable when considering the inaccuracy (regression slope = 0.37) and large negative bias (-177 W m^{-2}) of the flat-terrain interpolated LSHRG SWRAD data. Downscaled monthly and yearly SWRAD data are much more accurate than daily data and the monthly results indicate that HRCD captures seasonal SWRAD patterns fairly well.

Downscaled daily data for PRCP and WND matched observed distributions well and have very low RMSE and bias, even though the data do not correlate well (Figure 5 and Table 4). This inaccuracy is partially due to extremely high spatial and temporal variability of wind (Ha et al. 2009; Winstral et al. 2009) and precipitation (González-Hidalgo et al. 2001; Mock 1996) at short space and time scales. This variability cannot be represented by coarse-scale input, making it difficult to reconstruct in the fine-scale output (Tustison et al., 2001). However, HRCD captures seasonal and annual PRCP patterns fairly well, and has acceptable monthly and yearly PRCP accuracy while WND remains poorly estimated. HRCD also produces very good PRES values in the observed range of 810 hPa to 1050 hPa (GOF $R^2 = 0.987$, RMSE = 6.94 hPa, Bias = -1.58 hPa, regression slope = 0.965, n = 12706). In general, downscaled data accuracies improve with temporal aggregation to monthly and yearly values, except for decreased regression slopes for yearly values of SWRAD and WND and a zero regression slope for the constant DAY value across years (Table 4).

Using study-specific PRCP parameters (Table 1) dramatically improves downscaled monthly and yearly PRCP values and total number of PRCP days and negligibly affects SWRAD. No other variables are affected by these parameters. Figures 4 and 5 and table 4 present results based on study-specific parameter values. For comparison, the total number of observed precipitation days for 1998 - 2003 across sites was 7008, and the study-specific (initial) HRCD results were: PRCP days = 6895 (5143), PRCP monthly regression slope = 0.740 (0.629), PRCP monthly regression $r^2 = 0.691$ (0.67), PRCP monthly RMSE = 4 (4), PRCP monthly bias = 0 (-1), PRCP yearly regression slope = 0.825 (0.805), PRCP yearly RMSE = 19 (23), PRCP yearly bias = 5 (-

11). These results show that HRCD has sufficient parameterization flexibility to improve PRCP values when appropriate data are available.

Comparisons of HRCD, site-centered Daymet, and PRISM regressions against site observations show that HRCD performs as well as these other data sets with respect to DAY, SWRAD, TMAX, TMIN, and VPD (Table 4). PRISM, due to its sophisticated use of terrain in interpolation, performs equally well as Daymet on monthly and yearly bases with respect to sites. In general, HRCD is less accurate than Daymet and PRISM for PRCP, but HRCD monthly and yearly values are within a reasonable range. It is expected that Daymet and PRISM would estimate precipitation better than HRCD because they interpolate weather station measurements rather than gridded, $1^\circ \times 1^\circ$ resolution reanalysis data. These structural differences in input data likely influence HRCD PRCP accuracy because we selected the number of input cells required for elevation regression and PRCP occurrence (Table 1) based on Daymet analysis (Thornton et al. 1997) and statistical robustness. This incorporates distant input cells (up to ~ 300 km away) into these calculations, although a great circle distance-based Gaussian weighting function reduces the influence of more distant cells on regression. We also used only the four nearest-neighbor cells for interpolation to mitigate the effects of distance on the results. Using less input cells for these calculations further restricts the area of influence and might improve PRCP estimates. Nonetheless, the advantages of HRCD over PRISM are daily outputs and five additional variables. The advantages of HRCD over Daymet are gridded outputs, three additional variables, and nearly three times the historical range of data. The advantages of HRCD over both are the global extent, grid specification, and potential for generating high-resolution, spatially

gridded data from coarse resolution climate model projections. Thus, HRCD offers, with comparable accuracy, more variables and more flexible temporal and spatial grids than existing data sets.

3.2. Evaluations against site-relevant PRISM data

Evaluating HRCD and PRISM-centered Daymet data against site-related PRISM data extended our analyses to demonstrate very good regressions between Daymet-like algorithms and a very good, existing, gridded data set (Table 5). HRCD produced excellent results with respect to site-related PRISM data for TMAX, TMIN, and VPD, and good data for PRCP (Figure 6). Monthly and yearly results have comparable accuracies (Table 5). Comparisons of HRCD and PRISM-centered Daymet regressions against site-related PRISM data demonstrate that HRCD and Daymet data perform similarly well for TMAX, TMIN, and VPD, but, as expected, Daymet gives better results for PRCP. Given the previously stated advantages of HRCD over Daymet, these results demonstrate that HRCD would be a better candidate for producing very good, high-resolution, gridded climate variable data.

3.3. Evaluating HRCD against a 5° x 5° extent PRISM sub-grid

PRISM data correlates well with site observations, and accuracy comparisons of HRCD with Daymet and PRISM are consistent with respect to site and PRISM data (Tables 4 and 5). Thus, we further demonstrate the spatial robustness of HRCD accuracy through comparisons with a 5° x 5° sub-grid of PRISM data.

HRCD generates good PRCP data and very good TMAX, TMIN, and VPD data with respect to the PRISM sub-grid (Figure 7 and Table 6), even though these accuracies are not as high as those for the site-related comparisons (Figure 6 and Table 5). A slight decrease in accuracy might be expected because this gridded data set includes highly varied, complex terrain and a sample size three orders of magnitude larger than the one used for site observations.

However, irregular spreads on the scatter plots suggest that 2.5 arcmin resolution is too coarse to adequately capture all the topography within this region. Examination of the spatial distribution of precipitation error reveals the limitations associated with scale mismatch between $1^\circ \times 1^\circ$ daily precipitation rate data and fine spatial and temporal scales of rain events. Figure 8 shows a typical example of the spatial distribution of HRCD monthly PRCP error in relation to PRISM reference data. In general, HRCD underestimates high reference PRCP and overestimates low reference PRCP. This is partly due to the limited variability represented by the input data (Tustison et al., 2001) and partly due to the method for reducing unrealistically high PRCP. The dependency on input-point neighborhoods points is also apparent. The circular patterns indicate the dominance of particular 24-cell neighborhoods on the PRCP regression and occurrence, and the grid pattern delineates interpolation areas defined by four nearest-neighbor input cell centers. Given these data and methodological limitations, we did not expect highly accurate spatial results for PRCP, yet they are sufficient to produce good statistical accuracies for monthly estimates (Figures 5 – 7, Table 4).

Similar comparisons for monthly TMAX, TMIN, and VPD show less effects of the four-neighbor interpolation, and, as expected, the ranges of downscaled values are subsets of the

ranges of PRISM values, with some exceptions for TMIN. As with PRCP, lower variability in the input data causes HRCD to underestimate high reference TMAX and VPD, and overestimate low reference TMAX and VPD (Figures 9 and 10). The TMIN differences follow this pattern at extreme high/low reference values, but do not for other values. This is possibly due to temperature inversions that influence the downscaling and increase the variability of the results (Figure 11). In contrast to PRCP, we expected and generated high spatial fidelity for TMAX, TMIN, and VPD, with finer spatial structure than PRISM, and the statistical accuracies were very good to excellent for daily, monthly, and yearly estimates (Figures 4 – 7, Table 4). Nonetheless, reducing the number of regression points might improve estimates by restricting the input data to a more local region.

Furthermore, the site data used to determine the adequacy of this resolution are biased toward accessible areas (cities and towns) with low topographic variation. Downscaling to finer initial resolution and aggregating to 2.5 arcmin might increase accuracies given that HRCD output resolutions coarser than 2.5 arcmin did not correspond at all with aggregated PRISM data while aggregation of 2.5 arcmin HRCD output up to 15 arcmin maintained good relationships between HRCD and PRISM data (data not shown). HRCD consistently underestimates extreme precipitation events because of the parameterization to limit unrealistically high values (eqn. 1 and Table 1). Thus, the monthly PRCP regression is skewed by a minority of monthly totals greater than 20 cm, which indicates that in most cases HRCD performs better than the overall statistics. The statistics for yearly values generally show slight decreases in accuracies compared to monthly values, which likely results from averaging data exhibiting high seasonal variability

that is better captured monthly (Table 6).

3.4. Multi-scale evaluations against two sites

Comparisons of daily HRCD values with site observations showed inconsistent, generally negligible, changes in accuracies as resolution decreased to 1°. The changes were inconsistent partially because a different group of 2.5 arcmin cells was associated with a site for each aggregated resolution analysis. The 5° x 5° extent boundary was constant across resolutions, causing each site's location to shift relative to its aggregated cell boundary. Otherwise, one might expect a more consistent pattern as the aggregation more closely represents the area while the site becomes less representative of the area (Tustison et al. 2001). The only consistent result was that the gridded Desert Rock data were more accurate than the gridded Los Angeles data, which might have been influenced by slightly discrete TMAX and TMIN observation values at Los Angeles (data not shown). Presumably, the few cases with larger accuracy deviations resulted from inclusion of data dissimilar to the original 2.5 arcmin site cell, which would increase data variance within an aggregated cell, and, as expected, give a value more representative of the larger area and less representative of the single evaluation point.

Monthly HRCD and PRISM values had consistent accuracy at resolutions finer than 30 arcmin, but unlike the daily values some monthly accuracies have shown signs of degradation (Tables 7 and 8). HRCD and PRISM VPD and PRISM TMIN have shown degradation at 30 arcmin and coarser resolutions, and PRISM TMAX and HRCD TMIN have shown degradation at 1°. For yearly values we could reasonably evaluate only PRCP, TMAX, and VPD, but not the

other variables due to their poor statistical results. HRCD VPD has shown degradation at 15 arcmin and coarser resolutions, PRISM VPD and TMAX have shown degradation at 30 arcmin and coarser resolutions, and HRCD and PRISM PRCP have shown degradation at 1°. It is possible that PRISM values degraded at finer resolution than HRCD values because PRISM input data are more locally constrained than HRCD input data. The reported degradation of both bias and RMSE with respect to site observations was expected as the aggregated cell area increases, due to mismatch between point and area data.

The discrepancy between daily and monthly accuracy degradation suggests, however, that time influences this mismatch. HRCD is a terrain-dependent algorithm, and we can conclude that some of the degradation is due to averaging topographic effects. However, if terrain captured all the relevant spatial heterogeneity, we would expect the daily values to degrade similarly to the monthly values due to point-area mismatch. Even though the daily and monthly data are averaged across the same terrain, only a few daily cases show any degradation at all. This indicates that factors other than topography, such as land use/cover or clouds, might influence local climate at daily time scales. This dependence on non-terrain factors would increase the variance of the downscaled daily results, potentially reducing accuracy sufficiently to reduce the degrading effects of scale on results.

3.5. Evaluation against input data

Aggregating HRCD output to match input LSHRG cells demonstrates that sub-cell spatial heterogeneity is a determining factor of coarse-scale values. We have already shown HRCD's

downscaling success, and expect that aggregating accurate fine-scale values would give more accurate estimates of coarse-scale values than estimates based on less fine-scale data (Riley et al., 2009; Di Vittorio and Miller, in review). Furthermore, coarse-scale model outputs generally have biases often resulting from lack of finer-scale information, which has led to a variety of bias-correction techniques for statistical downscaling of precipitation (Anandhi et al. 2008; Boé et al. 2007). HRCD uses fine-scale topographic information to compensate for such biases by reducing scale mismatch between coarse-scale input and fine-scale output. Thus, supporting our expectation, bias and RMSE of HRCD outputs in relation to LSHRG inputs are greater than or equal to those in relation to site and PRISM data (Tables 4 - 6 and Table 9). Only the TMIN comparison for a subset of two sites has a larger absolute bias at any resolution, and this is likely due to the extreme topography in the region (Table 7). As expected, regressions for LWRAD, TMAX, TMIN, and VPD are good, albeit with high scatter, and for PRCP are poor (Table 9). Given the generally high accuracy of 2.5 arcmin HRCD outputs, the departure of aggregated HRCD outputs from LSHRG inputs indicates that fine-scale information has been successfully incorporated into the aggregated estimates, potentially improving their representativeness in relation to the LSHRG data, which was obtained by downscaling even coarser resolution data.

In common with other statistical downscaling techniques, HRCD does not conserve mass and energy with respect to input LSHRG data. This is not a problem when applying downscaled results to land processes uncoupled from the atmosphere because the main downscaling goal is higher accuracy with higher resolution. Statistical methods are calibrated to empirical data to give good results, obviating the need for physical consistency between scales, but also

precluding high-resolution land-atmosphere feedback studies. Regional dynamical downscaling maintains physical consistency for feedback studies, but can suffer from poorly represented processes and the effects of matching fine-scale processes to coarse-scale boundary conditions (Miller et al. 2009).

3.6 Caveats and limitations

HRCD provides good high-resolution meteorological forcings in the United States when using historical, daily LSHRG data. HRCD is implemented to easily accept other input data sources, but outputs based on additional sources would have to be evaluated prior to further application. Furthermore, the presented precipitation downscaling configuration is likely applicable only to the conterminous United States. The systematic negative bias (-54% for the 11 grid evaluation) introduced to the input data is latitude dependent, and the precipitation parameters have been tuned to the study sites. Even so, HRCD potentially overestimates precipitation. This overestimation likely results from a combination of factors inherent in the original DAYMET formulation. One factor is that the statistically sufficient number of points for regression and probability of precipitation calculations might cover an area too large to adequately capture local patterns. Another factor is the exclusion of non-precipitation input points to the modified cosine interpolation. This exclusion is meant to prevent artificially low precipitation values, but in HRCD it might cause artificially high precipitation values because only four, widely-spaced input points are available. Including non-precipitation points in the interpolation would likely reduce precipitation output values and cause the current bias-

correction method to be incorrect.

HRCD has been designed to avoid the assumption of temporal stationarity, and succeeds because statistical relationships are developed at each time step of the input data. This approach is robust at sub-geologic time scales, but it might not be applicable across tens of thousands of years because of the assumption that topography does not change. Furthermore, the physical basis of the precipitation bias-correction is valid at sub-astronomical time scales. On the other hand, common bias-correction methods are based on empirical data, but assume temporal stationarity. Thus, we did not explore bias-correction further. But, as indicated above, further exploration of the precipitation method is warranted due to its regional specificity, and this includes consideration of systematic bias correction. Bias-correction would also need to be addressed when applying HRCD to global and regional climate model projections, especially since it would likely require the assumption of temporal stationarity.

We do not directly address scale mismatch because we determined a sufficient match between 2.5 arcmin cell areas and our study sites, but our results highlight the importance of recognizing the limitations of spatial and temporal data sets with respect to scale. We compare HRCD outputs, representing areas, with both point and gridded data. The gridded data are more appropriate for comparison, but the point data are more accurate. Our multi-scale analysis against point data was used primarily to compare the effects of aggregation on HRCD and PRISM outputs, but it also indicates scale thresholds for divergence from a randomly selected point observation within a grid cell area. Consistent accuracy across scales finer than a divergence threshold could be a useful metric for determining the coarsest scale representative of

an area, when only sparse point data are available for evaluation. Determining this threshold is a practical application of minimizing error due to scale mismatch, or what Tustison et al. (2001) formalized as representativeness error. These relationships are further complicated by spatial heterogeneity in the time scale of biophysical processes that affect accuracies of daily, monthly, and yearly estimates.

4. Conclusions

We have successfully adapted and implemented a terrain-based point data technique for downscaling gridded data. HRCD performs very good downscaling of daily, global, historical $1^\circ \times 1^\circ$ resolution reanalysis data to 2.5 arcmin resolution with respect to DAY, LWRAD, TMAX, TMIN, and VPD. It gives good results for monthly and yearly PRCP and fair results for modeled SWRAD. The distributions of downscaled daily, monthly, and yearly PRCP and WND data are very good even though the daily values are poorly estimated. PRCP, VPD, TMAX, and TMIN are best estimated when adjusted for local topography, and PRCP can be improved by calibrating parameters to locally or regionally appropriate data sets. The parameters used in this study might be applicable only to the conterminous U.S. or the corresponding latitude belt. Monthly averaging of daily values generally improves accuracies, but yearly averaging can increase or decrease accuracies, which suggests that spatial and seasonal variability is better captured monthly. Based on 17 sites across the U.S., 2.5 arcmin resolution is sufficiently fine to accurately represent climate data at point sites within a grid cell. But HRCD comparison with a $5^\circ \times 5^\circ$ PRISM sub-grid suggests that finer resolution might be required to maintain accuracy across

complex terrain. The accuracy, with respect to a particular site, of coarser-resolution grids (created by aggregating 2.5 arcmin data) varies by variable and temporal averaging period, and might also vary by location, but more research is needed to determine this due to uncertainties associated with point-area mismatch. Terrain is most likely the limiting factor for accuracy of aggregated HRCD cells, and monthly averages suggest using resolutions finer than or equal to 15 arcmin. PRCP accuracy is also highly influenced by bias-correction and the number/location of input points used for regression and occurrence.

HRCD performs comparably to two existing gridding methods and has advantages over both. Daymet and PRISM generally have more accurate PRCP, and Daymet has more accurate SWRAD. But HRCD can generate global terrestrial, gridded, daily outputs for nine variables (DAY, LWRAD, PRCP, PRES, SWRAD, TMAX, TMIN, VPD, and WND) spanning 1948 - 2006. Additionally, HRCD can readily be applied to surface climate projections from global and regional climate models, once the appropriate PRCP parameters and bias-correction method are determined.

Overall, application of a simple, adapted point-based interpolation method to cell-based data provides good high-resolution, cell-based results. Our method assumes that topography is the primary factor affecting spatial variation in climate variable data, and that input data represent entire cell areas rather than individual points. Not surprisingly, terrain plays a major role in determining output accuracy and limits of interpolated and aggregated grid resolutions.

It is important to note that all the sites in this study are in or near cities and farmland, which suggests that sites in general might be biased toward accessible areas with gentle topography or

low elevations. Further analysis with careful site selection and experimental design is required to adequately assess HRCD accuracy across scales. More general applicability of HRCD also needs to be determined by comparing results from different historical and projected input climate data sets in additional regions and comparing HRCD results with outputs from dynamical and other statistical methods.

Acknowledgements

The Energy Biosciences Institute funded this research under grant EB107-J120. The ISLSCP Initiative II elevation data are courtesy of Kristen Verdin, the United States Geological Survey, and the Eros data center. Work performed at Lawrence Berkeley National Laboratory, including manuscript revision, was supported by the Director, Office of Science, Office of Basic Energy Sciences, of the U.S. Department of Energy under contract No. DE-AC02-05CH11231.

Appendix A. Modified cosine interpolation

Modified cosine interpolation is more consistent with cell-based data than other interpolation methods because it more heavily weights the nearest input point with respect to the quadrant containing the output point rather than calculating a weight based on a linear distance from the input point. HRCD uses a fourth-power cosine function to constrain input values to the four nearest-neighbor cells and to mitigate input cell boundary effects on the interpolated surface (Zhao et al. 2005):

$$D_i = \cos^4 \left[\left(\frac{\pi}{2} \right) \cdot \left(\frac{d_i}{d_{imax}} \right) \right] \quad i=1,2,3,4 \quad (\text{A1})$$

$$W_i = \frac{D_i}{\sum_{i=1}^4 D_i} \quad (\text{A2})$$

$$V = \sum_{i=1}^4 (W_i \cdot V_i) , \quad (\text{A3})$$

where i is the index of one of four nearest-neighbor input cell centers, D_i is the nonlinear distance between the output cell center and input cell center i (dimensionless), d_i is the great-circle distance between the output cell center and input cell center i (m), d_{imax} is the great-circle distance--passing through the output cell center--from input cell center i to the latitude-longitude boundary defined by the four nearest-neighbor input cell centers (m), W_i is the interpolation weight for input cell center i (dimensionless), V_i is the climate variable value at input the cell center i , and V is the interpolated climate variable value at the output cell center (Figure A1).

This d_{imax} constrains weights by the latitude-longitude boundary defined by the four nearest-neighbor input cell centers. Zhao et al. (2005) defines d_{imax} as the maximum great-circle distance

between any two of the four input cell centers. Thus, $D_i = W_i = 0$ only when the output cell center lies on the great circle associated with $d_{i_{\max}}$. In all other cases, with distortion increasing with latitude due to meridian convergence, inappropriately high weights can occur because $d_{i_{\max}}$ extends beyond the latitude-longitude boundary defined by the four nearest-neighbor input cell centers. Our $d_{i_{\max}}$, however, ensures that D_i is based on the relative position of the interpolation point within the four input cell centers.

Appendix B. Humidity variable conversion

For the daily input data described in section 2.2, TDEW (°C) is calculated from pressure and specific humidity via average vapor pressure using the inverse of the Magnus-Tetens formula (Campbell and Norman 1998):

$$e = 610.70 \cdot \exp\left(\frac{17.38 \cdot TDEW}{TDEW + 239.0}\right)$$

(B1)

and

$$e = \frac{PRES \cdot SH}{\left(\frac{M_{wv}}{M_{da}} \cdot (1 - SH)\right) \cdot \left(1 + \frac{SH}{\frac{M_{wv}}{M_{da}} \cdot (1 - SH)}\right)}, \quad (B2)$$

where e is the average vapor pressure (Pa), PRES is the input average surface pressure (Pa), SH is the average specific humidity (kg water vapor (kg (dry air + water vapor)⁻¹), M_{wv} is the molecular mass of water vapor (18.0148x10⁻³ kg mol⁻¹), and M_{da} is the molecular mass of dry air (28.9644x10⁻³ kg mol⁻¹).

After interpolation, TDEW is converted back to e using eqn. 2 and then converted to VPD by (Pa):

$$VPD = e_s - e \quad (B3)$$

and

$$TDAY = 0.725 \cdot TMAX + 0.275 \cdot TMIN, \quad (B4)$$

where e_s is the average saturation vapor pressure (Pa) calculated by eqn. (2) with TDAY (°C)

in place of TDEW, and TMAX and TMIN are maximum and minimum daily temperatures, respectively (°C). We also used eqns. (B1), (B3), and (B4) to convert verification data (Section 2.3) to VPD.

When TAVG and PRES input data are available, elevation-adjusted PRES is estimated by the hypsometric equation (Holton, 1992):

$$Z_2 - Z_1 = \frac{RT}{g} \cdot \ln \left[\frac{P_1}{P_2} \right] \quad (\text{B5})$$

The elevation-adjusted PRES is used with eqns. (B1) -(B4) to calculate an output SH.

References

- Anandhi A, Srinivas VV, Nanjundiah RS, Kumar DN (2008) Downscaling precipitation to river basin in India for IPCC SRES scenarios using support vector machine. *Int J Clim* 28 (3):401-420
- Aronoff S (2005) Remote sensing for GIS managers. ESRI Press, Redlands, CA
- Bayliss JL, Simonite V, Thompson S (2005) The use of probabilistic habitat suitability models for biodiversity action planning. *Agric, Ecosyst Environ* 108 (3):228-250
- Boé J, Terray L, Habets F, Martin E (2007) Statistical and dynamical downscaling of the Seine basin climate for hydro-meteorological studies. *Int J Clim* 27 (12):1643-1655
- Cabeza M, Arponen A, Jäättelä L, Kujala H, Teeffelen Av, Hanski I (2010) Conservation planning with insects at three different spatial scales. *Ecography* 33 (1):54-63
- Campbell GS, Norman JM (1998) An Introduction to Environmental Biophysics. 2nd edn. Springer, New York, New York
- Charles SP, Bates BC, Whetton PH, Hughes JP (1999) Validation of downscaling models for changed climate conditions: case study of southwestern Australia. *Clim Res* 12 (1):1-14
- Cheng CS, Li G, Li Q, Auld H (2008) Statistical downscaling of hourly and daily climate scenarios for various meteorological variables in South-central Canada. *Theor Appl Clim* 91 (1-4):129-147
- Daly C, Gibson WP, Taylor GH, Johnson GL, Pasteris P (2002) A knowledge-based approach to the statistical mapping of climate. *Clim Res* 22 (2):99-113
- Daly C, Neilson RP, Phillips DL (1994) A Statistical-Topographic Model for Mapping Climatological Precipitation over Mountainous Terrain. *J Appl Meteorol* 33 (2):140-158
- Daymet (2009) Daily surface weather data and climatological summaries, <http://www.daymet.org>. Accessed 2009
- Di Vittorio AV, Anderson RS, White JD, Miller NL, Running SW (2010) Development and optimization of an Agro-BGC ecosystem model for C4 perennial grasses. *Ecol Model* 221 (17):2038-2053
- Galatowitsch S, Frelich L, Phillips-Mao L (2009) Regional climate change adaptation strategies for biodiversity conservation in a midcontinental region of North America. *Biol Conserv* 142 (10):2012-2022
- Giorgi F, Shields Brodeur C, Bates GT (1994) Regional Climate Change Scenarios over the United States Produced with a Nested Regional Climate Model. *J Clim* 7 (3):375-399
- Girvetz EH, Thorne JH, Berry AM, Jaeger JAG (2008) Integration of landscape fragmentation analysis into regional planning: A statewide multi-scale case study from California, USA. *Landscape Urban Plann* 86 (3-4):205-218
- González-Hidalgo JC, Luis MD, Raventós J, Sánchez JR (2001) Spatial distribution of seasonal rainfall trends in a western Mediterranean area. *Int J Clim* 21 (7):843-860
- Ha K-J, Shin S-H, Mahrt L (2009) Spatial Variation of the Regional Wind Field with Land-Sea Contrasts and Complex Topography. *J Appl Meteorol Clim* 48 (9):1929-1939
- Hastings DA, Dunbar PK (1999) Global land one-kilometer base elevation (GLOBE) digital

elevation model, documentation, volume 1.0. vol Key to Geophysical Records Documentation (KGRD) 34. National Oceanic and Atmospheric Administration National Geophysical Data Center, 325 Broadway, Boulder, Colorado 80303, U.S.A.

- Hewitson BC, Crane RG (1996) Climate downscaling: techniques and application. *Clim Res* 07 (2):85-95
- Hijmans RJ, Cameron SE, Parra JL, Jones PG, Jarvis A (2005) Very high resolution interpolated climate surfaces for global land areas. *Int J Clim* 25 (15):1965-1978
- Holton JR (1992) An introduction to dynamic meteorology. 3rd edn. Academic Press, San Diego
- Iribane JV, Godson WL (1981) Atmospheric Thermodynamics, 2nd edn. D. Reidel Publishing Company, Dordrecht, The Netherlands
- Isaaks EH, Srivastava RM (1989) An introduction to applied geostatistics. Oxford University Press, New York, New York
- Jarvis A, Reuter HI, Nelson A, et al. (2008) Hole-filled SRTM for the globe Version 4, CGIAR CSI SRTM 90m Database. International Center for Tropical Agriculture, Cali, Columbia. <http://srtm.csi.cgiar.org>
- Jensen JR (2005) Introductory digital image processing: a remote sensing perspective. Prentice-Hall Series in Geographic Information Science, 3rd edn. Pearson Prentice Hall, Upper Saddle River, NJ
- Kalnay E, Kanamitsu M, Kistler R, Collins W, Deaven D, Gandin L, Iredell M, Saha S, White G, Woollen J, Zhu Y, Leetmaa A, Reynolds R, Chelliah M, Ebisuzaki W, Higgins W, Janowiak J, Mo KC, Ropelewski C, Wang J, Jenne R, Joseph D (1996) The NCEP/NCAR 40-Year Reanalysis Project. *B Am Meteorol Soc* 77 (3):437-471
- Kimball JS, Running SW, Nemani R (1997) An improved method for estimating surface humidity from daily minimum temperature. *Agr Forest Meteorol* 85 (1-2):87-98
- Kucharik CJ, Foley JA, Delire C, Fisher VA, Coe MT, Lenters JD, Young-Molling C, Ramankutty N, Norman JM, Gower ST (2000) Testing the performance of a dynamic global ecosystem model: Water balance, carbon balance, and vegetation structure. *Global Biogeochem Cy* 14 (3):795-825
- Landman WA, Tennant WJ (2000) Statistical downscaling of monthly forecasts. *Int J Clim* 20 (13):1521-1532
- Lo JCF, Yang ZL, Pielke RA (2008) Assessment of three dynamical climate downscaling methods using the Weather Research and Forecasting (WRF) model. *J Geophys Res-Atmos* 113 (D09112)
- Maurer EP, Hidalgo HG, Das T, Dettinger MD, Cayan DR (2010) The utility of daily large-scale climate data in the assessment of climate change impacts on daily streamflow in California. *Hydrol Earth Syst Sci* 14 (6):1125-1138
- Ma S, Baldocchi DD, Xu L, Hehn T (2007) Inter-annual variability in carbon dioxide exchange of an oak/grass savanna and open grassland in California. *Agric For Meteorol* 147:157-171
- Maurer EP, Wood AW, Adam JC, Lettenmaier DP, Nijssen B (2002) A Long-Term Hydrologically Based Dataset of Land Surface Fluxes and States for the Conterminous United States. *J Clim* 15 (22):3237-3251
- Mesinger F, DiMego G, Kalnay E, Mitchell K, Shafran PC, Ebisuzaki W, Jovifá Da, Woollen J,

- Rogers E, Berbery EH, Ek MB, Fan Y, Grumbine R, Higgins W, Li H, Lin Y, Manikin G, Parrish D, Shi W (2006) North American Regional Reanalysis. *B Am Meteorol Soc* 87 (3):343-360
- Miguez FE, Zhu X, Humphries S, Bolero GA, Long SP (2009) A semimechanistic model predicting the growth and production of the bioenergy crop *Miscanthus giganteus*: description, parameterization and validation. *GCB Bioenergy* 1 (4):282-296
- Miller NL, Cayan D, Duffy P, Hidalgo H, Jin J, Kanamaru H, Kanamitsu M, O'Brien T, Schlegel N, Sloan L, Snyder M, Yoshimura K (2009) An analysis of simulated CA climate using multiple dynamical and statistical techniques. The California Climate Change Center Report Series. CEC-500-2009-017-F
- Mitchell TD, Jones PD (2005) An improved method of constructing a database of monthly climate observations and associated high-resolution grids. *Int J Clim* 25 (6):693-712
- Mock CJ (1996) Climatic Controls and Spatial Variations of Precipitation in the Western United States. *J Clim* 9 (5):1111-1125
- Paul S, Liu CM, Chen JM, Lin SH (2008) Development of a statistical downscaling model for projecting monthly rainfall over East Asia from a general circulation model output. *J Geophys Res-Atmos* 113 (D15)
- PRISM-Climate-Group (2010) Oregon State University, Created 4 Feb 2004, <http://www.prismclimate.org>. Accessed 2010
- Richards JA (1993) Remote sensing digital image analysis: an introduction. Springer-Verlag, Berlin
- Riley WJ, Biraud SC, Torn MS, Fischer ML, Billesbach, DP, Berry JA (2009) Regional CO₂ and latent heat surface fluxes in the Southern Great Plains: Measurements, modeling, and scaling. *J Geophys Res* 114 (G04009):1-15
- Running SW, Coughlan JC (1988) A general model of forest ecosystem processes for regional applications I. Hydrologic balance, canopy gas exchange and primary production processes. *Ecol Model* 42 (2):125-154
- Running SW, Nemani RR, Hungerford RD (1987) Extrapolation of synoptic meteorological data in mountainous terrain and its use for simulating forest evapotranspiration and photosynthesis. *Can J Forest Res* 17 (6):472-483
- Salathe EP, Mote PW, Wiley MW (2007) Review of scenario selection and downscaling methods for the assessment of climate change impacts on hydrology in the United States pacific northwest. *Int J Clim* 27 (12):1611-1621
- Schubert S (1998) Downscaling local extreme temperature changes in south-eastern Australia from the CSIRO Mark2 GCM. *Int J Clim* 18 (13):1419-1438
- Sheffield J, Goteti G, Wood EF (2006) Development of a 50-year high-resolution global dataset of meteorological forcings for land surface modeling. *J Clim* 19 (13):3088-3111
- Shepard D (1968) A two-dimensional interpolation function for irregularly-spaced data. Proceedings of the 1968 23rd Association for Computing Machinery (ACM) National Conference. ACM, New York, NY, USA. DOI: 10.1145/800186.810616
- Spak S, Holloway T, Lynn B, Goldberg R (2007) A comparison of statistical and dynamical

- downscaling for surface temperature in North America. *J Geophys Res-Atmos* 112 (D8)
- Steinacker R, Ratheiser M, Bica B, Chimani B, Dorninger M, Gepp W, Lotteraner C, Schneider S, Tschannett S (2006) A mesoscale data analysis and downscaling method over complex terrain. *Mon Weather Rev* 134 (10):2758-2771
- Sylla MB, Gaye AT, Pal JS, Jenkins GS, Bi XQ (2009) High-resolution simulations of West African climate using regional climate model (RegCM3) with different lateral boundary conditions. *Theor Appl Clim* 98 (3-4):293-314
- Tao K, Barros AP (2010) Using Fractal Downscaling of Satellite Precipitation Products for Hydrometeorological Applications. *J Atmos Ocean Tech* 27 (3):409-427
- Thornton PE, Hasenauer H, White MA (2000) Simultaneous estimation of daily solar radiation and humidity from observed temperature and precipitation: an application over complex terrain in Austria. *Agr Forest Meteorol* 104 (4):255-271
- Thornton PE, Rosenbloom NA (2005) Ecosystem model spin-up: Estimating steady state conditions in a coupled terrestrial carbon and nitrogen cycle model. *Ecol Model* 189 (1-2):25-48
- Thornton PE, Running SW, White MA (1997) Generating surfaces of daily meteorological variables over large regions of complex terrain. *J Hydrol* 190 (3-4):214-251
- Tustison B, Harris D, Foufoula-Georgiou E (2001) Scale issues in verification of precipitation forecasts. *J Geophys Res* 106 (D11):1775-11784
- Trigo RM, Palutikof JP (2001) Precipitation scenarios over Iberia: A comparison between direct GCM output and different downscaling techniques. *J Clim* 14 (23):4422-4446
- Wilby RL, Wigley TML (1997) Downscaling general circulation model output: a review of methods and limitations. *Prog Phys Geog* 21 (4):530-548
- Wilby RL, Wigley TML, Conway D, Jones PD, Hewitson BC, Main J, Wilks DS (1998) Statistical downscaling of general circulation model output: A comparison of methods. *Water Resour Res* 34 (11):2995-3008
- Winstral A, Marks D, Gurney R (2009) An efficient method for distributing wind speeds over heterogeneous terrain. *Hydrol Process* 23 (17):2526-2535
- Zhang XC (2005) Spatial downscaling of global climate model output for site-specific assessment of crop production and soil erosion. *Agr Forest Meteorol* 135 (1-4):215-229
- Zhao M, Heinsch FA, Nemani RR, Running SW (2005) Improvements of the MODIS terrestrial gross and net primary production global data set. *Remote Sens Environ* 95 (2):164-176

Figure captions

Figure 1. Flow chart of the High Resolution Climate Downscaler (HRCD) algorithm.

Figure 2. Map of 17 United States weather stations used in this study (Table 2). Black text denotes 11 National Climatic Data Center (NCDC) stations and dark gray text denotes 6 Surface Radiation (SURFRAD) network stations.

Figure 3. Map of $5^{\circ} \times 5^{\circ}$ region of the southwestern United States used for grid-based evaluations over complex terrain. The thick black line separates California on the left from Nevada on the right. The thin black lines are county boundaries. The black area is the Pacific Ocean and the grayscale values represent maximum temperature on 1 Jan. 2003 with 2.5 arcmin resolution.

Figure 4. Scatter plots of daily, downscaled (2.5 arcmin resolution) values versus station observations. Data span 1998 - 2003 and observations are from 6 to 17 stations depending on data availability. The downscaled data coincide with Parameter-elevation Regressions on Independent Slopes Model (PRISM) grid cells containing the stations. Reg. r^2 is the regression line coefficient of determination, GOF (R^2) is the coefficient of determination for the downscaled values, and RMSE is the Root Mean Squared Error.

Figure 5. Histograms and scatter plots of downscaled (2.5 arcmin resolution) values versus station observations for precipitation and average wind speed. Histograms present daily data and scatter plots present monthly data. Histograms do not include data for days with zero precipitation or zero average wind speed. Data span 1998 - 2003 and observations are from 11 and 17 stations for precipitation and average wind speed, respectively. The downscaled data coincide with Parameter-elevation Regressions on Independent Slopes Model (PRISM) grid cells containing the stations. Reg. r^2 is the regression line coefficient of determination, GOF (R^2) is the coefficient of determination for the downscaled values, and RMSE is the Root Mean Squared Error.

Figure 6. Scatter plots of 2.5 arcmin resolution monthly downscaled values versus Parameter-elevation Regressions on Independent Slopes Model (PRISM) values corresponding to 17 weather stations. Data span 1998 - 2003 and the downscaled data coincide with PRISM grid cells containing the 17 stations. Reg. r^2 is the regression line coefficient of determination, GOF (R^2) is the coefficient of determination for the downscaled values, and RMSE is the Root Mean Squared Error.

Figure 7. Scatter plots of 2.5 arcmin resolution monthly downscaled values versus Parameter-elevation Regressions on Independent Slopes Model (PRISM) values across a $5^{\circ} \times 5^{\circ}$ region of the southwestern United States (Figure 3). Data span 1998 - 2003 and the downscaled data

coincide with PRISM grid cells. Reg. r^2 is the regression line coefficient of determination, GOF (Goodness of Fit) R^2 is the coefficient of determination for the downscaled values, and RMSE is the Root Mean Squared Error.

Figure 8. Typical comparison of monthly precipitation (PRCP) at 2.5 arcmin resolution for a $5^\circ \times 5^\circ$ region of the southwestern United States (Figure 3). These data are from April, 2001; a) High Resolution Climate Downscaler (HRCD) - Parameter-elevation Regressions on Independent Slopes Model (PRISM); b) PRISM; c) HRCD. Note that neutral gray has a value of 0 cm.

Figure 9. Typical comparison of monthly maximum temperature (TMAX) at 2.5 arcmin resolution for a $5^\circ \times 5^\circ$ region of the southwestern United States (Figure 3). These data are from April 2001; a) High Resolution Climate Downscaler (HRCD) - Parameter-elevation Regressions on Independent Slopes Model (PRISM); b) PRISM; c) HRCD. Note that neutral gray has a value of 0°C .

Figure 10. Typical comparison of monthly vapor pressure deficit (VPD) at 2.5 arcmin resolution for a $5^\circ \times 5^\circ$ region of the southwestern United States (Figure 3). These data are from April 2001; a) High Resolution Climate Downscaler (HRCD) - Parameter-elevation Regressions on Independent Slopes Model (PRISM); b) PRISM; c) HRCD. Note that a value of 0 Pa is nearly black.

Figure 11. Typical comparison of monthly minimum temperature (TMIN) at 2.5 arcmin resolution for a $5^\circ \times 5^\circ$ region of the southwestern United States (Figure 3). These data are from April 2001; a) High Resolution Climate Downscaler (HRCD) - Parameter-elevation Regressions on Independent Slopes Model (PRISM); b) PRISM; c) HRCD. Note that neutral gray has a value of 0°C .

Figure A1. Modified cosine interpolation. In this study the output interpolation point is the center of the output cell. d_i is the great circle distance between input cell center i (1-4) and the output interpolation point. $d_{i\max}$ is the great circle distance between input cell center i and the latitude/longitude boundary defined by the four input cell centers, passing through the interpolation point.

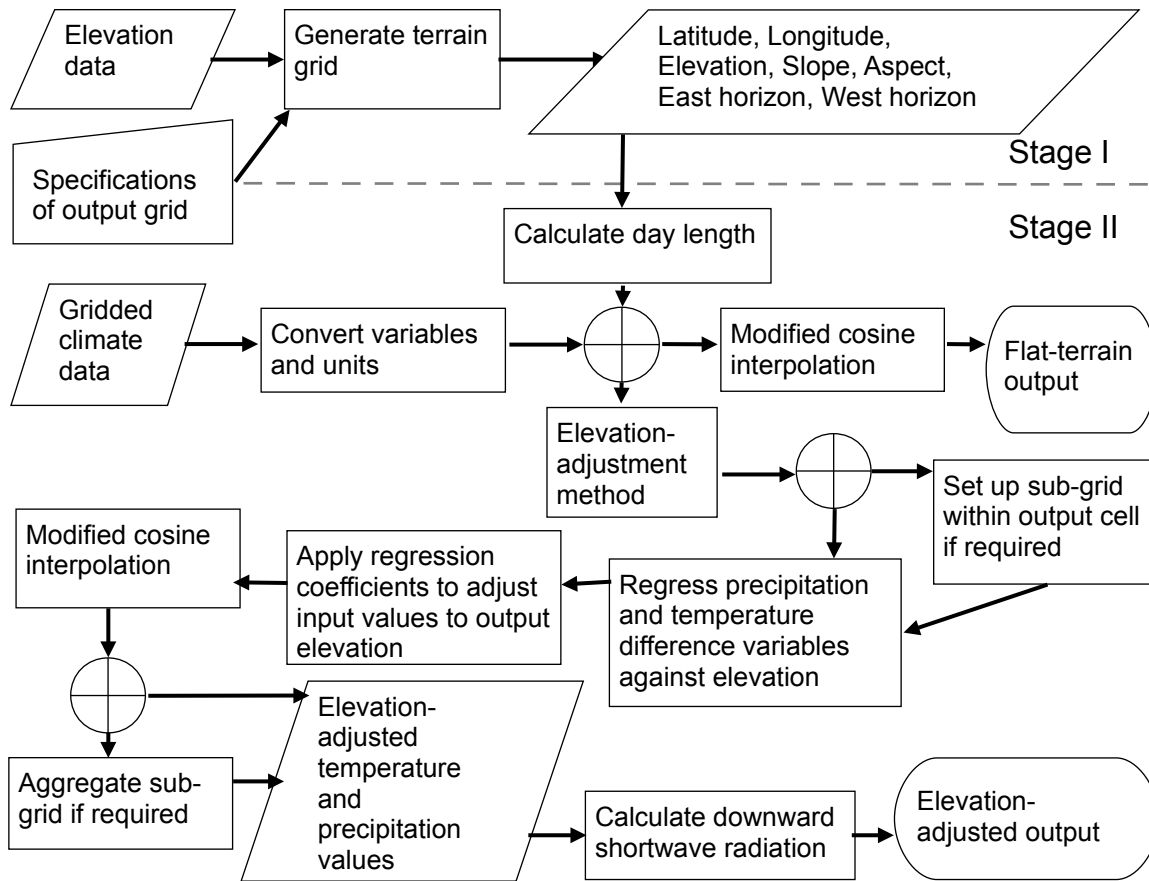


Figure 1

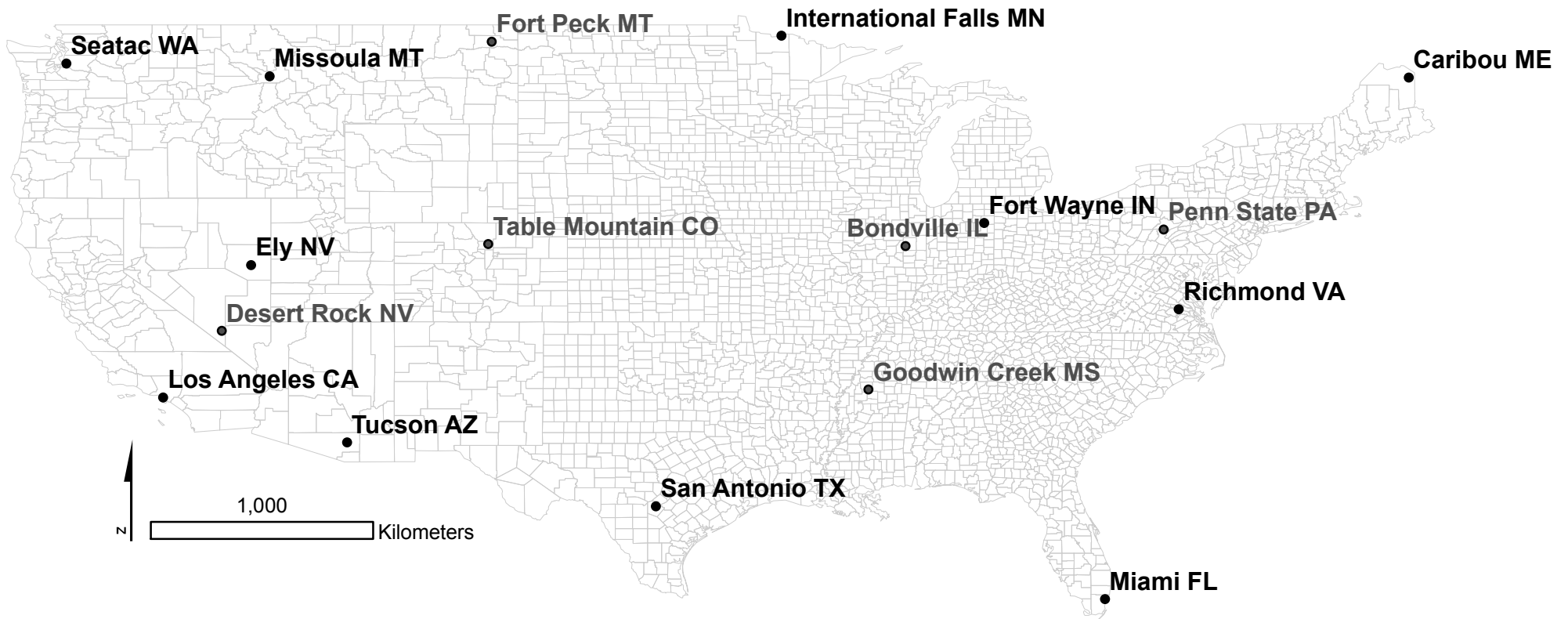


Figure 2

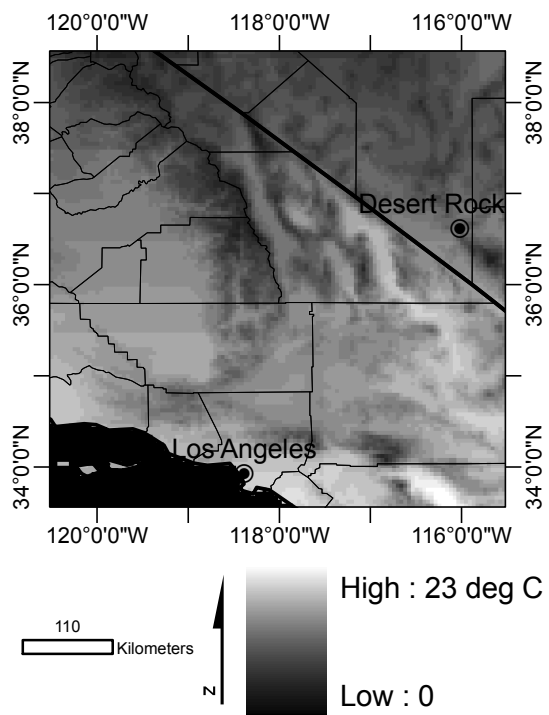
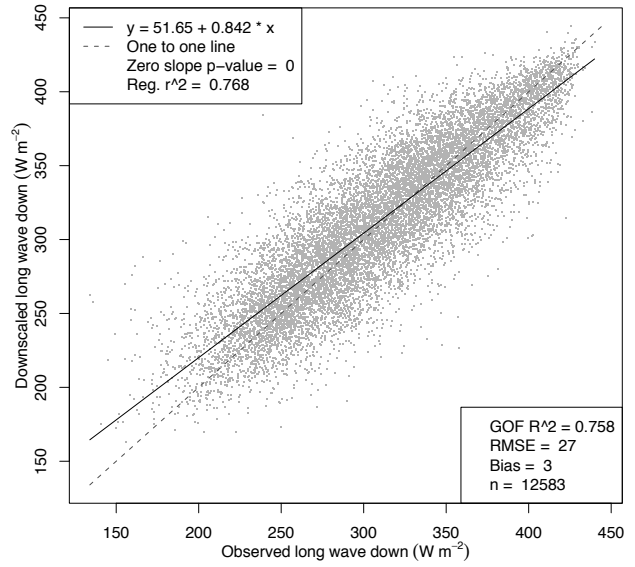
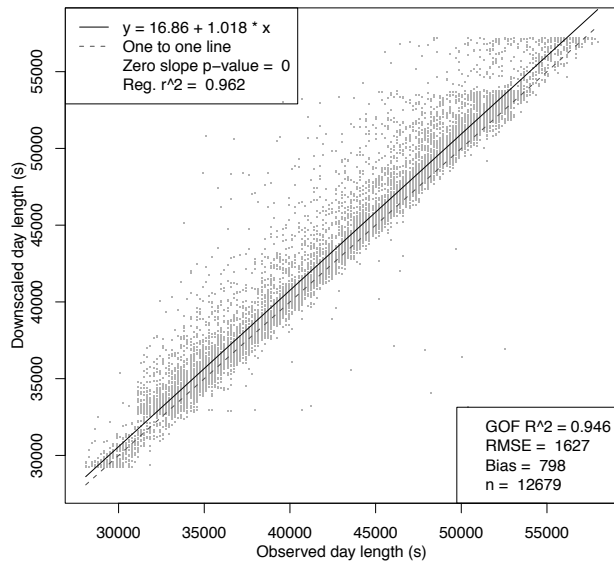


Figure 3

a) Day length

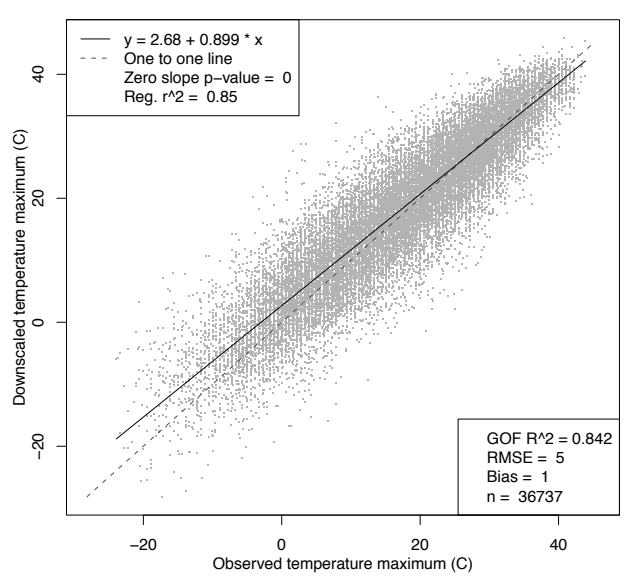
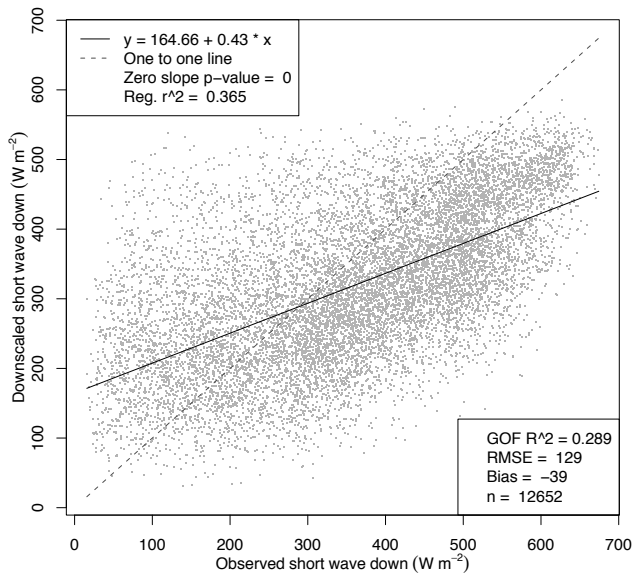
Figure 4

b) Longwave down



c) Shortwave down

d) Temperature maximum



e) Temperature minimum

f) Average vapor pressure deficit

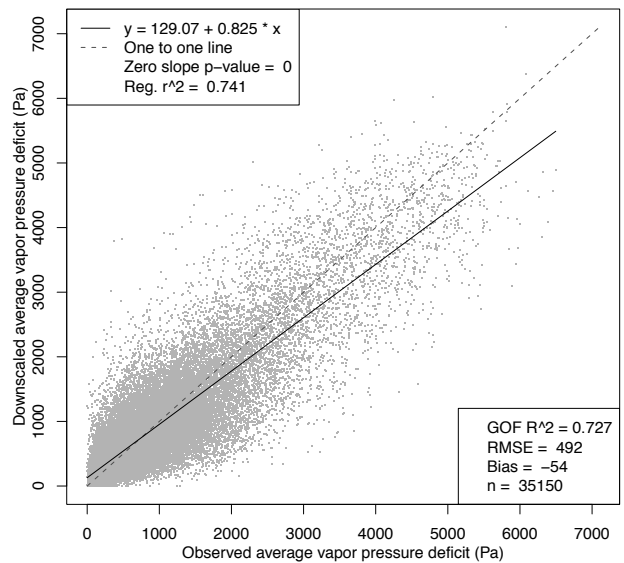
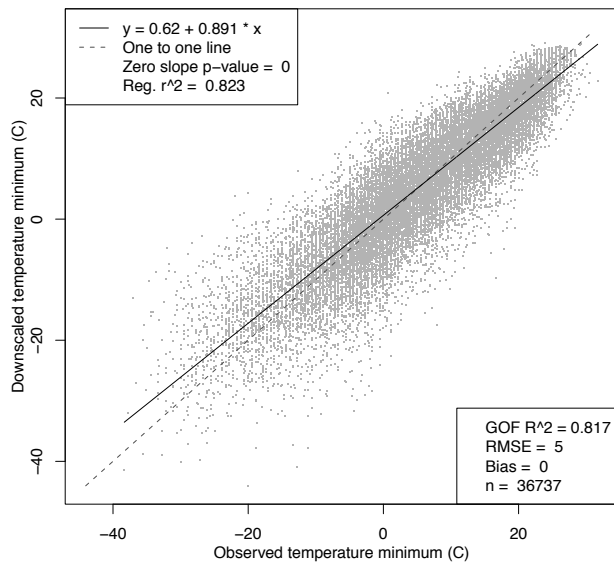


Figure 5

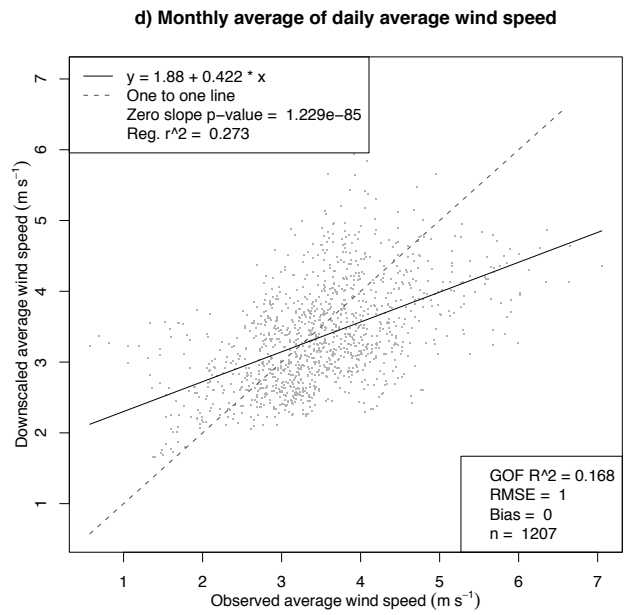
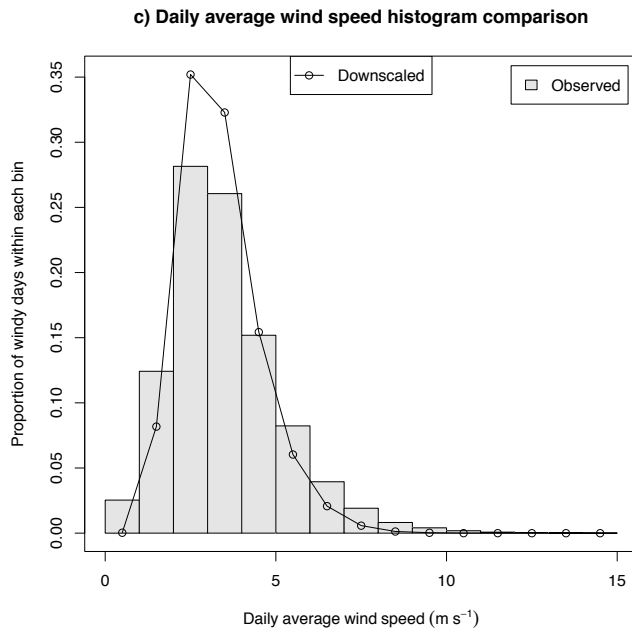
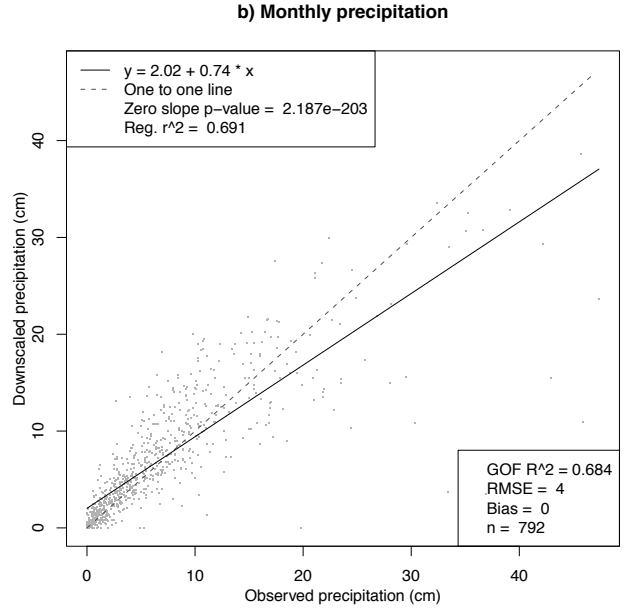
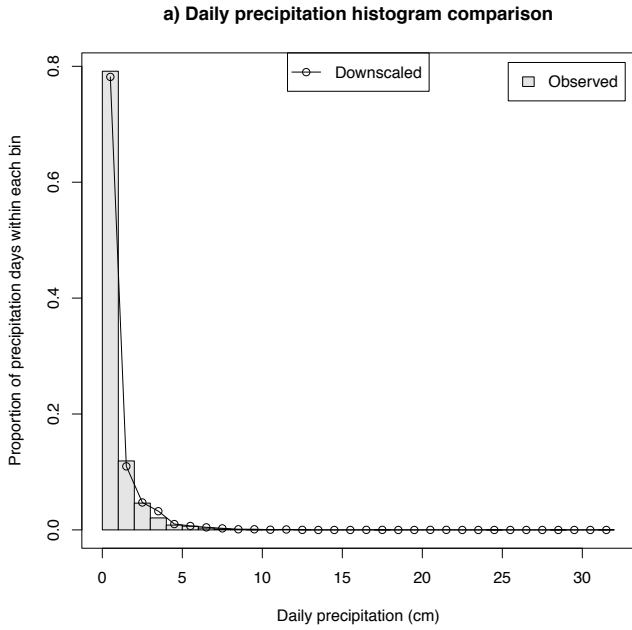


Figure 6

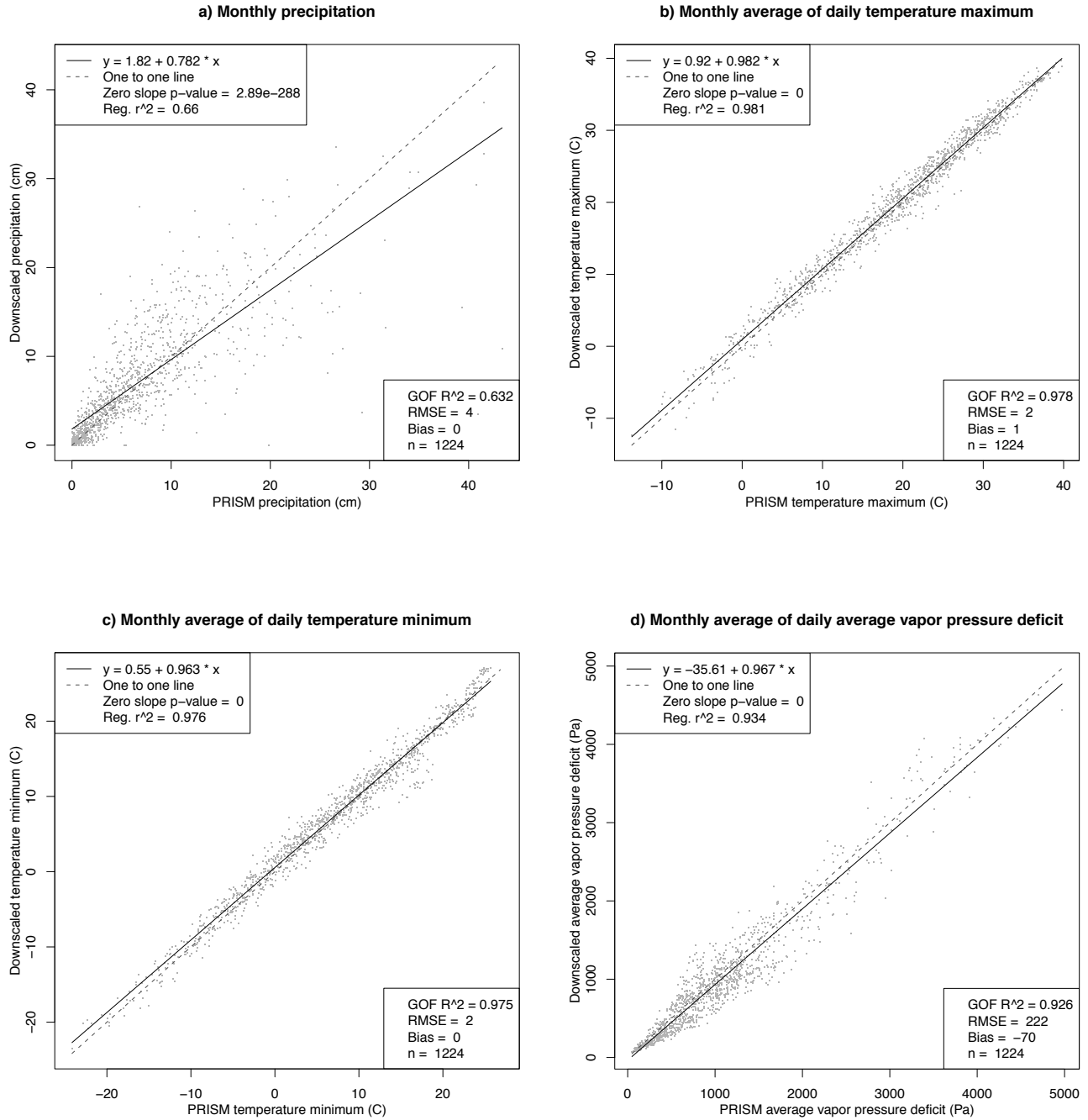
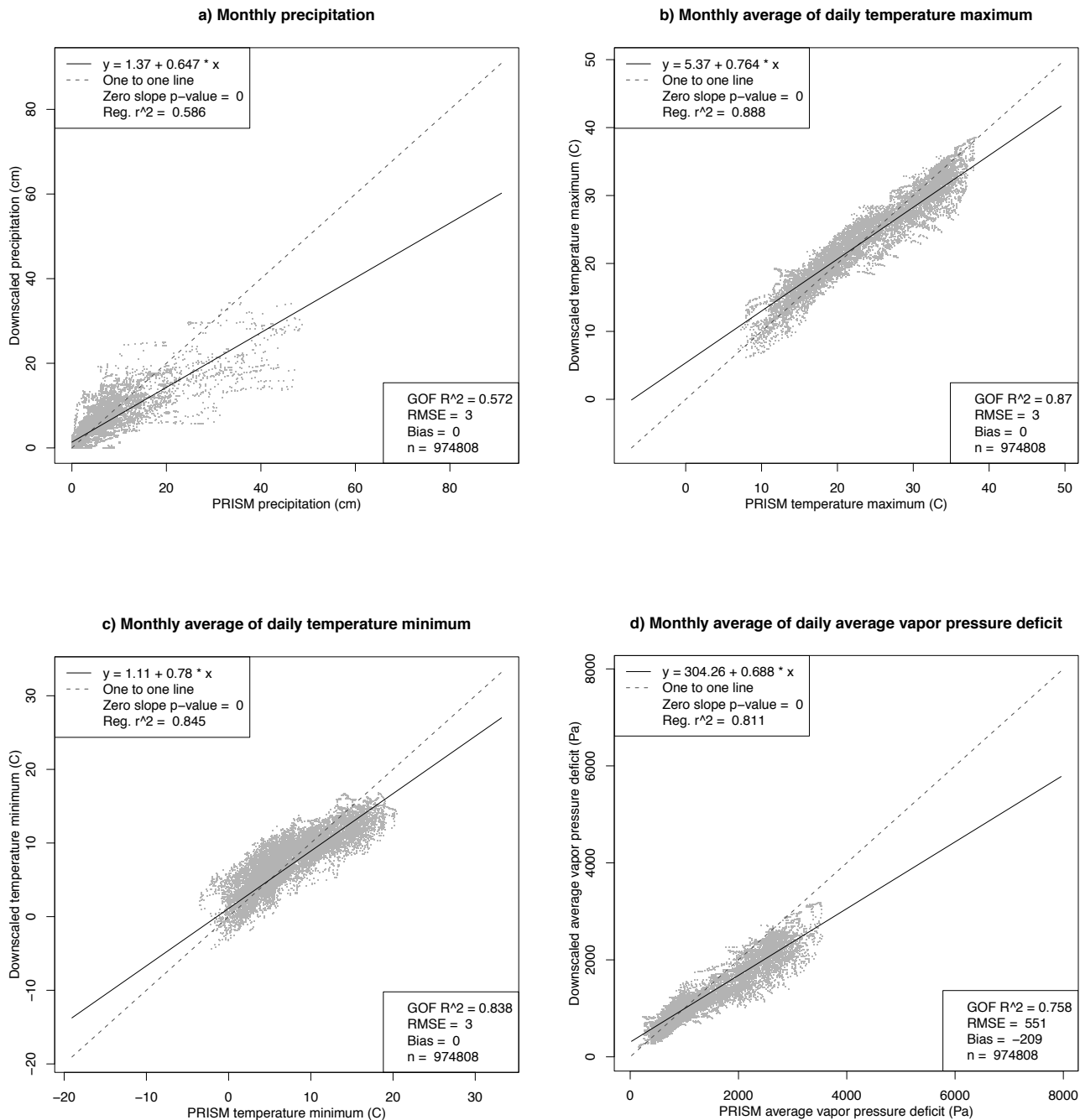


Figure 7



a) HRCD PRCP - PRISM PRCP

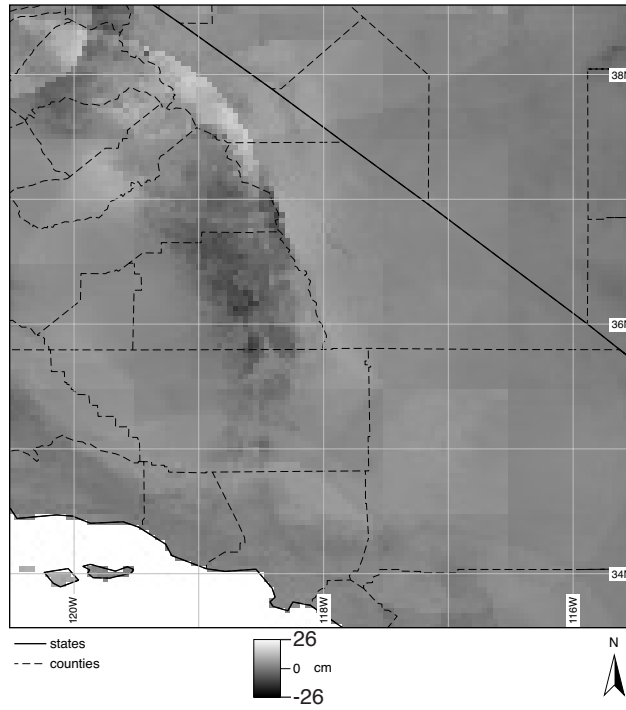
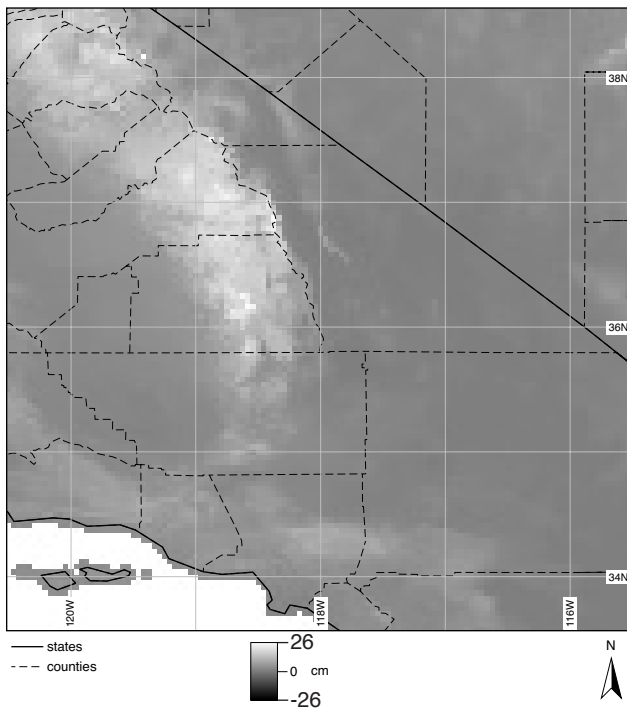
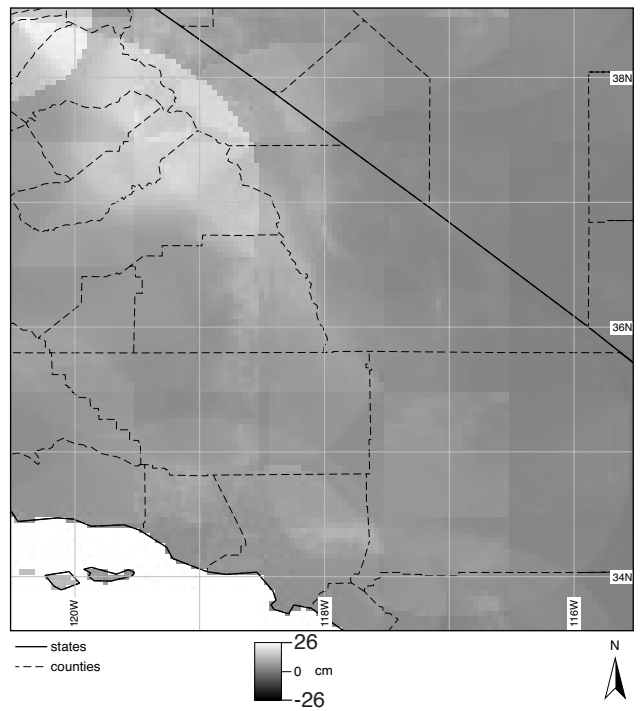


Figure 8

b) PRISM PRCP



c) HRCD PRCP



a) HRCD TMAX - PRISM TMAX

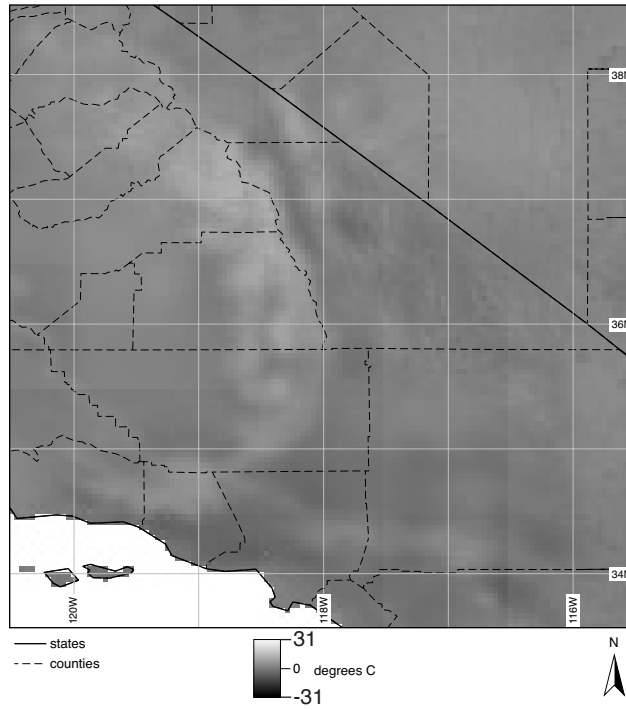
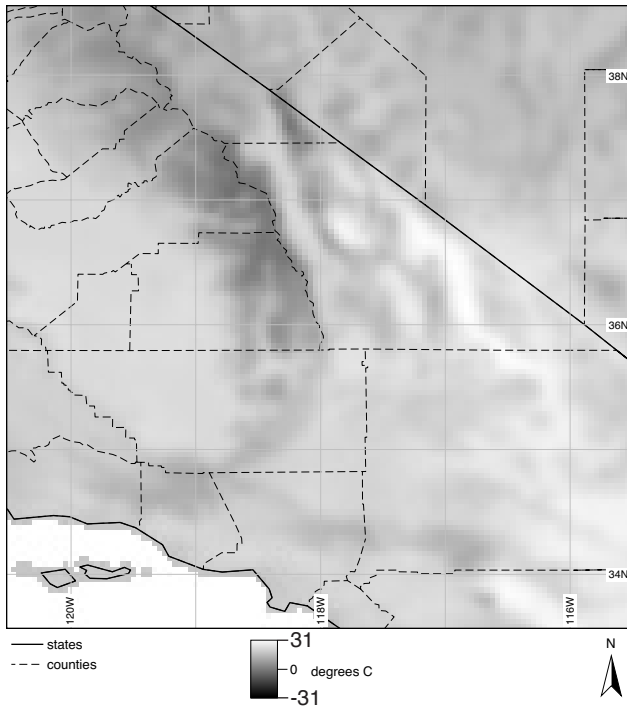
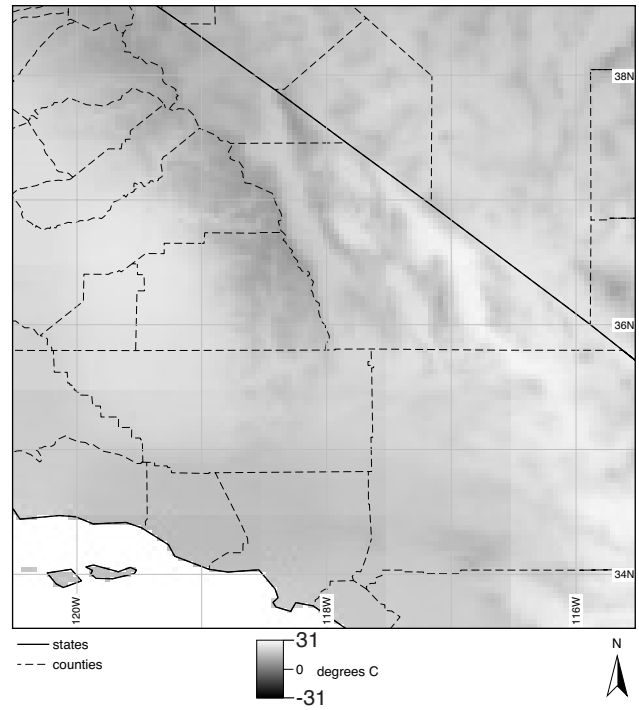


Figure 9

b) PRISM TMAX



c) HRCD TMAX



a) HRCD VPD - PRISM VPD

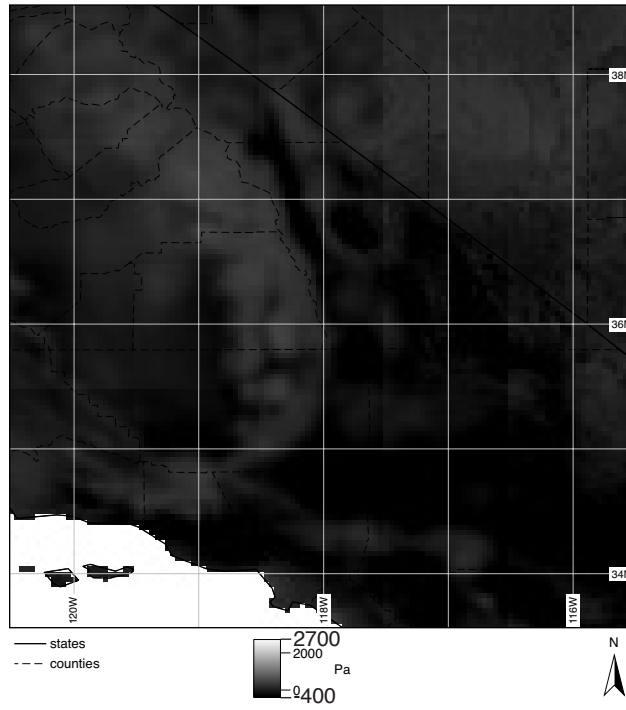
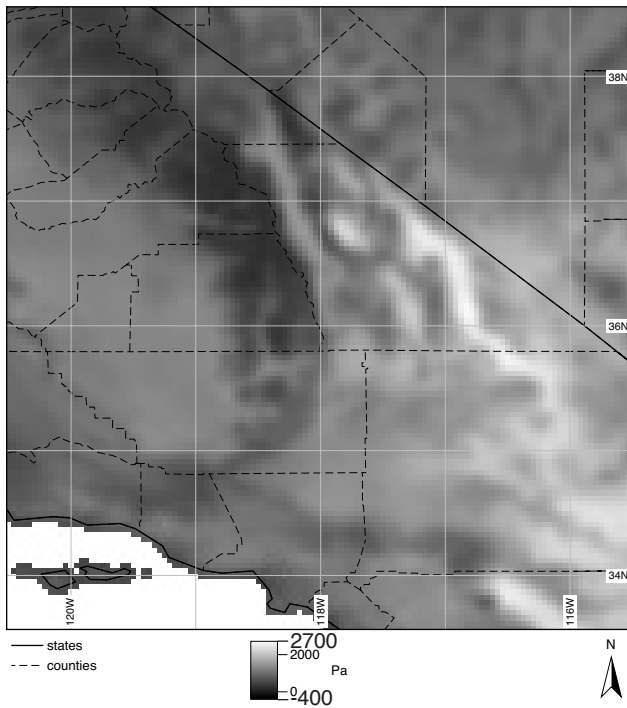
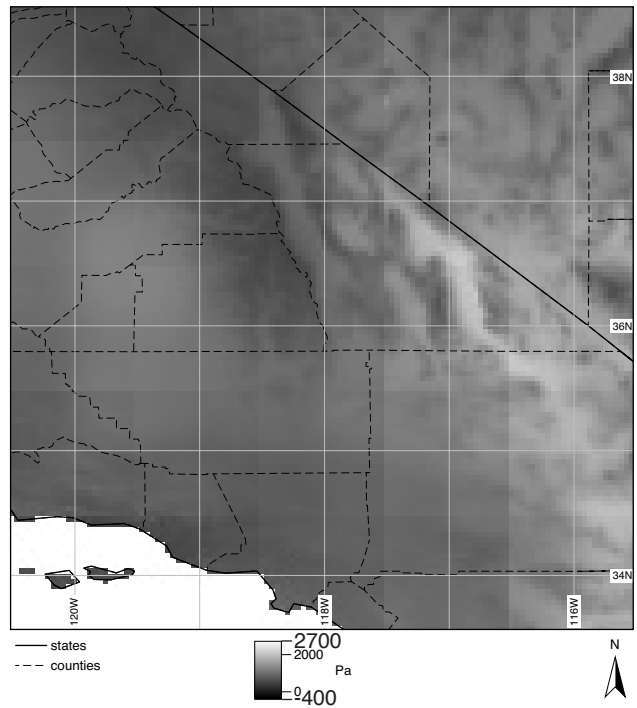


Figure 10

b) PRISM VPD



c) HRCD VPD



a) HRCD TMIN - PRISM TMIN

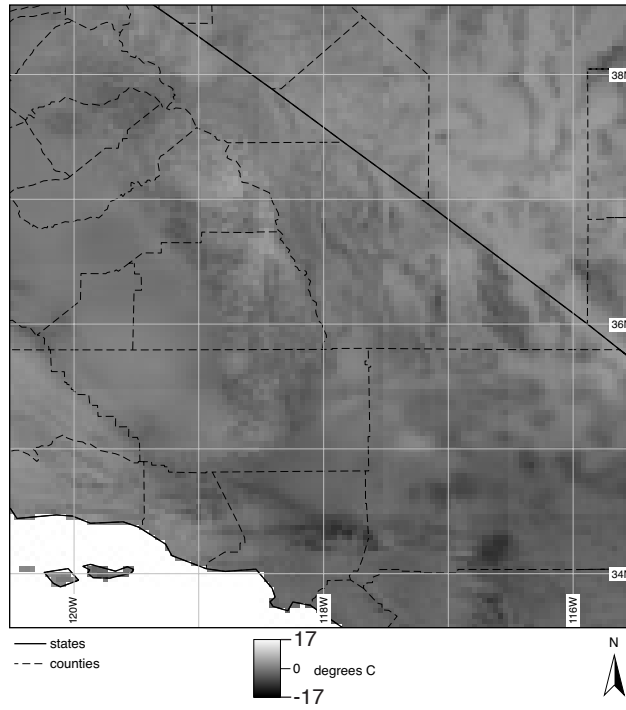
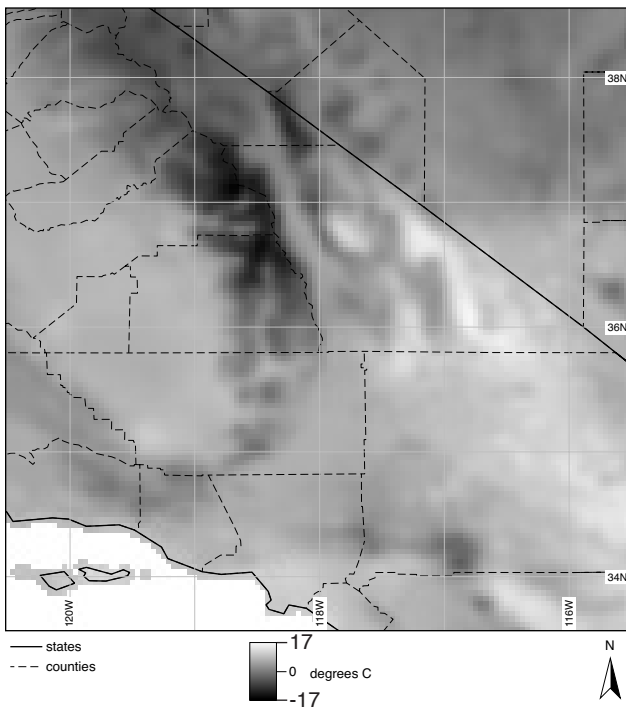
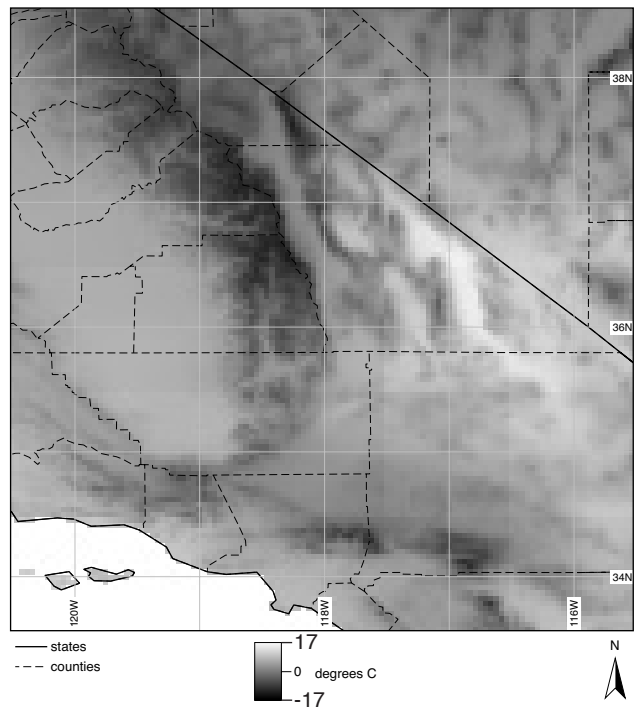


Figure 11

b) PRISM TMIN



c) HRCD TMIN



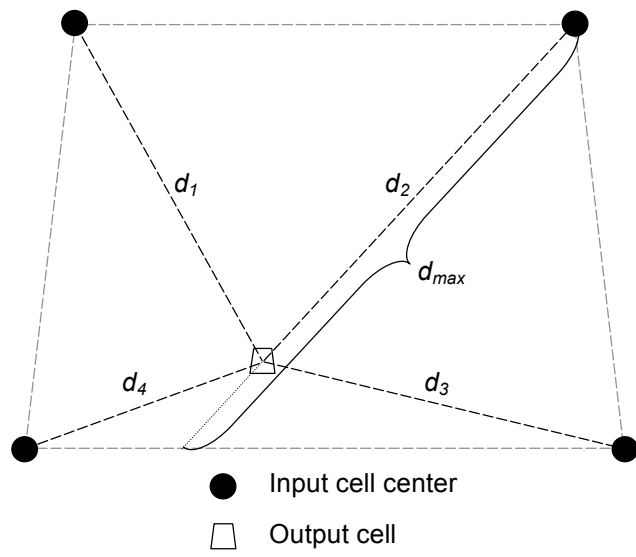


Figure A1

Table 1. Elevation-adjusted interpolation parameters for precipitation and temperature.

Parameter	Units	Value
Number of temperature regression points	None	32
Number of precipitation regression points	None	24
Temperature regression Gaussian shape parameter	None	3.4
Precipitation regression Gaussian shape parameter	None	7.6
Maximum value for magnitude of estimated precipitation ratio	None	0.95
Precipitation occurrence threshold (CRIT_POP) ^a	None	0.25 (0.36)
Extreme precipitation threshold (EXTR_PRCP) ^a	(cm)	4 (3)
Maximum precipitation reduction exponent (PRCP_REDUCE) ^a	None	0.5 (0.8)

^aNon-parenthetical values were determined from this study's site data and parenthetical values were originally determined during algorithm development using two non-study test sites.

Table 2. Weather station locations and elevations.

Site	Latitude (°)	Longitude (°)	Reported Elevation (m)	2.5 arcmin ^a Elevation (m)
NCDC ^b				
Caribou, Maine	46.86667	-68.01667	190	153
Ely, Nevada	39.28333	-114.83333	1909	1894
Fort Wayne, Indiana	40.98333	-85.18333	241	233
International Falls, Minnesota	48.55000	-93.38333	361	351
Los Angeles, California	33.93333	-118.38333	30	27
Miami, Florida	25.78333	-80.30000	9	4
Missoula, Montana	46.91667	-114.08333	973	983
Richmond, Virginia	37.50000	-77.31667	50	49
San Antonio, Texas	29.53333	-98.46667	247	245
Seatac, Washington	47.43333	-122.30000	113	92
Tuscon, Arizona	32.11667	-110.95000	777	766
SURFRAD ^c				
Bondville, Illinois	40.05	-88.37	213	212
Desert Rock, Nevada	36.62	-116.02	1007	1062
Fort Peck, Montana	48.31	-105.1	634	621
Goodwin Creek, Mississippi	34.25	-89.87	98	91
Penn State, Pennsylvania	40.72	-77.93	376	475
Table Mountain, Colorado	40.13	-105.24	1689	1649

^a2.5 arcmin grid resolution elevations were generated by the High Resolution Climate Downscaler (HRCD).

^bNational Climate Data Center (NCDC) cooperative network.

^cSURFace RADiation budget network (SURFRAD).

Table 3. Organization of data sets for presented statistical analyses.

Number of data sets	Base data set	Permutations
4	Regression against all site observations^a	
	F-tests between slopes and t-tests between biases for all combinations ^b	
2	HRCG 2.5 arcmin, PRISM-cell-centered, 1 interpolation point	Elevation-adjusted with humidity input Flat terrain
1	Daymet	Site-centered
1	PRISM ^d 2.5 arcmin	Cells containing sites
2	Regression against 2.5 arcmin PRISM cells containing sites	
	F-tests between slopes and t-tests between biases for all combinations ^e	
1	HRCG 2.5 arcmin, PRISM-cell-centered, elevation-adjusted with humidity input	1 interpolation point
1	Daymet	PRISM-centered
1	Regression against 5° x 5° extent aggregated PRISM grids^f	
	F-tests between slopes and t-tests between biases for all combinations ^e	
1	HRCG 2.5 arcmin, PRISM-matched, elevation-adjusted with humidity input	1 interpolation point
24	Regression against two sites within 5° x 5° extent grid	
	F-tests between slopes and t-tests between biases for all combinations ^{e,g}	
8	HRCG 2.5 arcmin, PRISM-centered, 1 interpolation point, elevation-adjusted with humidity input	aggregated to 2.5, 5, 7.5, 10, 12.5, 15, 30, and 60 arcmin cells
8	HRCG 2.5 arcmin, PRISM-centered, 1 interpolation point, flat terrain	aggregated to 2.5, 5, 7.5, 10, 12.5, 15, 30, and 60 arcmin cells
8	PRISM 2.5 arcmin cells contains sites	aggregated to 2.5, 5, 7.5, 10, 12.5, 15, 30, and 60 arcmin cells
1	Regression against 1° x 1° LSHRG input cells	
1	HRCG 2.5 arcmin, LSHRG-aligned, elevation-adjusted with humidity input	aggregated to 1 degree cells

^aSite data are from 17 weather stations (Table 2 and Figure 3).

^bThese tests were duplicated with original and new precipitation parameters (Table 1).

^cHigh Resolution Climate Downscaler (HRCG).

^dParameter-elevation Regressions on Independent Slopes Model (PRISM).

^eThese tests were done using new precipitation parameters only.

^fGrid area covers part of the southwestern United States (Figure 4).

^gSample sizes were mismatched across cell sizes.

Table 4. High Resolution Climate Downscaler (HRCD)^a, Daymet^b, and PRISM^c regressions (reg.) against combined data from 17 sites spanning 1998-2003.

Statistic	DAY ^d (s)	LWRAD ^e (W m ⁻²)	PRCP ^e (cm)	SWRAD ^e (W m ⁻²)	TMAX (°C)	TMIN (°C)	VPD (Pa)	WND ^e (m s ⁻¹)
Daily HRCD								
n	12679	12583	24076	12652	36737	36737	35150	36697
Reg. slope ^f	1.02	0.84	0.06*	0.43*	0.90*	0.89*	0.83*	0.36
Reg. r ²	.096	0.77	0.00	0.37	0.85	0.82	0.74	0.26
RMSE ^g	1627	27	1	129	5	5	492	1
Bias	798	3	0	-39*	1	0	-54*	0
Daily Daymet								
n	12679	-	24076	12652	36737	36737	35150	-
Reg. slope	1.02	-	0.64*	0.59*	0.97*	0.95*	0.88*	-
Reg. r ² (R ²) ^h	0.96	-	0.53	0.57 (0.55)	0.96	0.96	0.84	-
RMSE	1630	-	1	103	2	2	402	-
Bias	798	-	0	-22	1	-1	118*	-
Monthly HRCD								
n	418	410	792	417	1207	1207	1116	1207
Reg. slope	1.05	0.99	0.74*	0.70*	0.99*	0.96*	0.95	0.42
Reg. r ² (R ²)	0.99	0.96	0.69	0.82 (0.68)	0.98	0.97	0.94	0.27
RMSE	1068	10	4	62	2	2	224	1
Bias	796	3	0	-39*	1	0	-55*	0
Monthly Daymet								
n	418	-	792	417	1207	1207	1116	-
Reg. slope	1.05	-	1.00* [#]	0.84*	1.00*	0.97 [#]	0.94 [#]	-
Reg. r ² (R ²)	0.99	-	0.91	0.88 (0.83)	1.00	0.98	0.90	-
RMSE	1069	-	2	45	1	2	294	-
Bias	796	-	1	-22*	1	-1	115* [#]	-
Monthly PRISM								
n	-	-	792	-	1207	1207	1116	-
Reg. slope	-	-	0.94* [#]	-	1.01*	0.99* [#]	0.98 [#]	-
Reg. r ² (R ²)	-	-	0.96	-	1.00	0.99	0.99	-
RMSE	-	-	1	-	1	1	99	-
Bias	-	-	0	-	0	0	6 [#]	-
Yearly HRCD								
n	33	31	66	33	98	98	83	97
Reg. slope	0.00	0.96	0.83*	0.54	1.03*	0.91	1.02*	0.26
Reg. r ² (R ²)	0.00	0.87	0.85	0.91 (0.27)	0.99	0.97	0.97	0.15
RMSE	896	9	19	46	1	1	123	1
Bias	815	3	5	-38	1	0	-42	0
Yearly Daymet								
n	33	-	66	33	98	98	83	-
Reg. slope	0.00	-	1.04*	0.64	0.99*	0.92	0.88*	-
Reg. r ² (R ²)	0.15	-	0.95 (0.92)	0.87 (0.65)	1.00	0.95	0.92 (0.88)	-
RMSE	896	-	13	32	1	2	212	-
Bias	815	-	7	-21	1	-1	120 [#]	-
Yearly PRISM								
n	-	-	66	-	98	98	83	-
Reg. slope	-	-	1.00*	-	0.99*	0.96	0.89*	-
Reg. r ² (R ²)	-	-	1.00	-	0.99	0.97	0.97 (0.92)	-
RMSE	-	-	3	-	0	1	167	-
Bias	-	-	1	-	0	0	-117 [#]	-

^aHRCD 2.5 arcmin data, except flat-interpolated LWRAD and WND, were generated using elevation-adjusted interpolation with humidity input and one interpolation point at the center of PRISM cells containing the sites.

^bSite-centered Daymet data.

^cParameter-elevation Regressions on Independent Slopes Model.

^dDAY = day length, LWRAD = downward long wave radiation, PRCP = cumulative precipitation, SWRAD = downward short wave radiation, TMAX = temperature maximum, TMIN = temperature minimum, VPD = vapor pressure deficit, WND = wind speed.

^eHRCD PRCP and SWRAD data were generated using precipitation parameters determined with the site data in this study. For PRCP results based on original parameters see section 3.1.

SWRAD results were nearly identical for original and new parameters.

^fAll slopes are significantly non-zero ($p < 0.05$), except for HRCD yearly DAY.

^gRMSE = Root Mean Squared Error.

^hReg. r^2 is the coefficient of determination for the regression model, and R^2 is the coefficient of determination for the generated data. R^2 not shown if the difference is less than 0.02 or reg. $r^2 < 0.5$.

* $p < 0.05$ for slope or bias comparison between same HRCD and Daymet or PRISM variables within temporal scope.

$p < 0.05$ for slope or bias comparison between same Daymet and PRISM variables within temporal scope.

Table 5. High Resolution Climate Downscaler (HRCD)^a and Daymet^b regressions (reg.) against PRISM^c data for 17, 2.5 arcmin cells spanning 1998-2003.

Statistic	HRCD				Daymet			
	PRCP ^d (cm)	TMAX (°C)	TMIN (°C)	VPD (Pa)	PRCP (cm)	TMAX (°C)	TMIN (°C)	VPD (Pa)
Monthly (n = 1224)								
Reg. slope ^e	0.78*	0.98*	0.96*	0.97	1.06*	0.96*	0.98*	0.95
Reg. r ² (R ²) ^f	0.66 (0.63)	0.98	0.98	0.93	0.95 (0.93)	1.00	0.99	0.90
RMSE ^g	4	2	2	222	2	1	1	272
Bias	0	1	0	-70*	0	0	0	95*
Yearly (n = 102)								
Reg. slope	0.86*	1.04	0.94	1.12*	1.52*	1.00	0.96	0.95*
Reg. r ² (R ²) ^f	0.87	0.98	0.98	0.95	0.97 (0.91)	1.00	0.99	0.91 (0.71)
RMSE	17	1	1	152	10	0	1	271
Bias	5	1	0	55*	4	0	0	220*

^aHRCD data were generated using elevation-adjusted interpolation with humidity input and one interpolation point at the center of PRISM cells containing the sites.

^bPRISM cell-centered Daymet data.

^cParameter-elevation Regressions on Independent Slopes Model.

^dPRCP = cumulative precipitation, TMAX = temperature maximum, TMIN = temperature minimum, VPD = vapor pressure deficit.

^eAll slopes are significantly non-zero ($p < 0.05$).

^fReg. r² is the coefficient of determination for the regression model, and R² is the coefficient of determination for the generated data. R² not shown if the difference is less than 0.02 or reg. r² < 0.5.

^gRMSE = Root Mean Squared Error.

* $p < 0.05$ for slope or bias comparison between same HRCD and Daymet variables within temporal scope.

Table 6. High Resolution Climate Downscaler (HRCD)^a regressions (reg.) against PRISM^b data for a 5° x 5° grid with 2.5 arcmin resolution spanning 1998-2003.

Statistic	Monthly (n = 974808)				Yearly (n = 81234)			
	PRCP ^c (cm)	TMAX (°C)	TMIN (°C)	VPD (Pa)	PRCP (cm)	TMAX (°C)	TMIN (°C)	VPD (Pa)
Reg. slope ^d	0.65	0.76	0.78	0.69	0.55	0.61	0.75	0.58
Reg. r^2 (R^2) ^e	0.59 (0.57)	0.89 (0.87)	0.85	0.81 (0.76)	0.64 (0.60)	0.78 (0.72)	0.73	0.53
RMSE ^f	3	3	3	551	19	3	3	344
Bias	0	0	0	-209	5	0	0	-8

^aHRCD data were generated using elevation-adjusted interpolation with humidity input and one interpolation point at the center of PRISM cells containing the sites.

^bParameter-elevation Regressions on Independent Slopes Model.

^cPRCP = cumulative precipitation, TMAX = temperature maximum, TMIN = temperature minimum, VPD = vapor pressure deficit.

^dAll slopes are significantly non-zero ($p < 0.05$).

^eReg. r^2 is the coefficient of determination for the regression model, and R^2 is the coefficient of determination for the generated data. R^2 not shown if the difference is less than 0.02 or reg. $r^2 < 0.5$.

^fRMSE = Root Mean Squared Error.

Table 7. High Resolution Climate Downscaler (HRCD)^a regressions (reg.) against combined site data from Los Angeles, CA and Desert Rock, NV for selected resolutions spanning 1998-2003.

Statistic	Monthly data				Yearly data			
	TMIN (°C)		VPD (Pa)		PRCP ^b (cm)		VPD (Pa)	
n	139	139	139	139	6	6	11	11
Resolution	2.5	1°	2.5	30	2.5	1°	2.5	30
	arcmin		arcmin		arcmin		arcmin	
Reg. slope ^c	0.84	0.86	0.86	0.79	0.83	1.05	0.78	0.70
Reg. r^2 (R^2) ^d	0.90	0.91	0.96	0.96	0.94	0.96	0.99	0.99
	(0.83)	(0.18)		(0.93)	(0.89)	(0.61)	(0.95)	(0.90)
RMSE ^e	2	5	262	324	6	12	181	247
Bias	-2	-5	20	-51	4	11	20	-47

^aHRCD 2.5 arcmin data were generated using elevation-adjusted interpolation with humidity input and one interpolation point at the center of PRISM cells containing the sites. Lower resolutions were aggregated from the 2.5 arcmin data.

^bPRCP = cumulative precipitation, TMAX = temperature maximum, TMIN = temperature minimum, VPD = vapor pressure deficit.

^cAll slopes are significantly non-zero ($p < 0.05$).

^dReg. r^2 is the coefficient of determination for the regression model, and R^2 is the coefficient of determination for the generated data. R^2 not shown if the difference is less than 0.02 or reg. $r^2 < 0.5$.

^eRMSE = Root Mean Squared Error.

Table 8. PRISM^a regressions (reg.) against combined site data from Los Angeles, CA and Desert Rock, NV for selected resolutions spanning 1998-2003.

Statistic	Monthly (n = 139)					
	TMAX (°C) ^b		TMIN (°C)		VPD (Pa)	
Resolution	2.5 arcmin	1°	2.5 arcmin	30 arcmin	2.5 arcmin	30 arcmin
Reg. slope ^c	1.03	1.00	1.00	1.01	0.93	0.80
Reg. r ² (R ²) ^d	1.00	0.80 (0.75)	0.98 (0.95)	0.89 (0.72)	1.00	0.98 (0.94)
RMSE ^e	0	3	1	3	136	289
Bias	0	0	-1	-2	-66	-50
	Yearly					
	PRCP (cm)		TMAX (°C)		VPD (Pa)	
n	6	6	11	11	11	11
Resolution	2.5 arcmin	1°	2.5 arcmin	30 arcmin	2.5 arcmin	15 arcmin
Reg. slope ^c	0.95	0.98	1.01	0.38	0.71	0.64
Reg. r ² (R ²) ^d	1.00	0.94 (0.68)	1.00	0.90 (0.56)	1.00 (0.86)	1.00 (0.81)
RMSE ^e	1	11	0	1	297	343
Bias	0	9	0	0	-185	-194

^aParameter-elevation Regressions on Independent Slopes Model. Original 2.5 arcmin resolution data were aggregated to lower resolutions.

^bPRCP = cumulative precipitation, TMAX = temperature maximum, TMIN = temperature minimum, VPD = vapor pressure deficit.

^cAll slopes are significantly non-zero ($p < 0.05$).

^dReg. r² is the coefficient of determination for the regression model, and R² is the coefficient of determination for the generated data. R² not shown if the difference is less than 0.02 or reg. r² < 0.5.

^eRMSE = Root Mean Squared Error.

Table 9. Comparison of aggregated 2.5 arcmin HRCD^a results with LSHRG^b input data for 176, 1° x 1° cells spanning 5 years.

Statistic	PRCP ^c		LWRAD (W m ⁻²)	TMAX (°C)	TMIN (°C)	VPD (Pa)
	Daily (cm)	Monthly (cm)				
n	321200	10560	321200	321200	321200	321200
Reg. slope ^d	0.01	-0.05	0.87	0.89	0.92	0.98
Reg. r ²	0.00	0.00	0.40	0.62	0.38	0.12
RMSE ^e	0.98	8	46	7	8	756
Bias	0.08	2	18	0	1	241

^aHigh Resolution Climate Downscaler.

^bLand Surface Hydrology Research Group.

^cPRCP = cumulative precipitation, LWRAD = downward long wave radiation, TMAX = temperature maximum, TMIN = temperature minimum, VPD = vapor pressure deficit.

^dAll slopes are significantly non-zero ($p < 0.05$).

^eRMSE = Root Mean Squared Error.

DISCLAIMER

This document was prepared as an account of work sponsored by the United States Government. While this document is believed to contain correct information, neither the United States Government nor any agency thereof, nor The Regents of the University of California, nor any of their employees, makes any warranty, express or implied, or assumes any legal responsibility for the accuracy, completeness, or usefulness of any information, apparatus, product, or process disclosed, or represents that its use would not infringe privately owned rights. Reference herein to any specific commercial product, process, or service by its trade name, trademark, manufacturer, or otherwise, does not necessarily constitute or imply its endorsement, recommendation, or favoring by the United States Government or any agency thereof, or The Regents of the University of California. The views and opinions of authors expressed herein do not necessarily state or reflect those of the United States Government or any agency thereof or The Regents of the University of California.

Ernest Orlando Lawrence Berkeley National Laboratory is an equal opportunity employer.